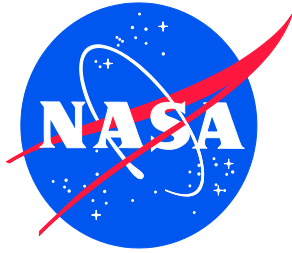


NASA/TM-20220001916



The Discontinuous Galerkin Finite Element Method

Ivatury S. Raju
Langley Research Center, Hampton, Virginia

February 2022

NASA STI Program Report Series

Since its founding, NASA has been dedicated to the advancement of aeronautics and space science. The NASA scientific and technical information (STI) program plays a key part in helping NASA maintain this important role.

The NASA STI program operates under the auspices of the Agency Chief Information Officer. It collects, organizes, provides for archiving, and disseminates NASA's STI. The NASA STI program provides access to the NTRS Registered and its public interface, the NASA Technical Reports Server, thus providing one of the largest collections of aeronautical and space science STI in the world. Results are published in both non-NASA channels and by NASA in the NASA STI Report Series, which includes the following report types:

- **TECHNICAL PUBLICATION.** Reports of completed research or a major significant phase of research that present the results of NASA Programs and include extensive data or theoretical analysis. Includes compilations of significant scientific and technical data and information deemed to be of continuing reference value. NASA counterpart of peer-reviewed formal professional papers but has less stringent limitations on manuscript length and extent of graphic presentations.
- **TECHNICAL MEMORANDUM.** Scientific and technical findings that are preliminary or of specialized interest, e.g., quick release reports, working papers, and bibliographies that contain minimal annotation. Does not contain extensive analysis.
- **CONTRACTOR REPORT.** Scientific and technical findings by NASA-sponsored contractors and grantees.

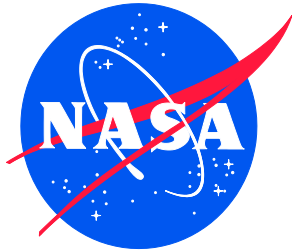
- **CONFERENCE PUBLICATION.** Collected papers from scientific and technical conferences, symposia, seminars, or other meetings sponsored or co-sponsored by NASA.
- **SPECIAL PUBLICATION.** Scientific, technical, or historical information from NASA programs, projects, and missions, often concerned with subjects having substantial public interest.
- **TECHNICAL TRANSLATION.** English-language translations of foreign scientific and technical material pertinent to NASA's mission.

Specialized services also include organizing and publishing research results, distributing specialized research announcements and feeds, providing information desk and personal search support, and enabling data exchange services.

For more information about the NASA STI program, see the following:

- Access the NASA STI program home page at <http://www.sti.nasa.gov>
- Help desk contact information: <https://www.sti.nasa.gov/sti-contact-form/> and select the "General" help request type.

NASA/TM-20220001916



The Discontinuous Galerkin Finite Element Method

Ivatury S. Raju
Langley Research Center, Hampton, Virginia

National Aeronautics and
Space Administration

Langley Research Center
Hampton, Virginia 23681-2199

February 2022

The use of trademarks or names of manufacturers in the report is for accurate reporting and does not constitute an official endorsement, either expressed or implied, of such products or manufacturers by the National Aeronautics and Space Administration.

Available from:

NASA STI Program / Mail Stop 148
NASA Langley Research Center
Hampton, VA 23681-2199
Fax: 757-864-6500

Preface

This work was performed during the COVID-19 pandemic of 2020. NASA computers were not available to the author because of the shutdown. As such, all the work was performed on a PC and without mainframe computers. However, the author found that his error rate was getting worse as the order of matrices was past 3! One late afternoon, the author arrived at his desktop computer disgusted with his errors, and asked Google if Excel can perform matrix operations. Lo and Behold! to his surprise Google's answer was a resounding YES. The author immediately asked Google to show the results of Excel matrix operations search. Excel showed that it can perform all matrix operations accurately and efficiently. All the computations presented in this report were performed on a PC using Excel.

Acknowledgements:

The author is deeply indebted to Le Ann (Dee) Bullock for all the help in getting this manuscript 'dressed up' as a NASA TM. She has been using her 'magic' on all our manuscripts for the past two plus decades.

Table of Contents

1.0	Introduction.....	6
2.0	Weighted Residual (WR) Methods.....	6
3.0	Weak Form.....	14
4.0	Discontinuous Galerkin Finite Element Method	20
5.0	EXAMPLES	39
6.0	Concluding Remarks	58
7.0	References.....	59
	Appendix A.....	61

List of Figures

Figure 1.	Various idealizations.....	16
Figure 2.	Cantilever and simply supported beam problems studied.	39
Figure 3.	Various idealizations for cantilever and simply supported beam problems.	44
Figure 4.	Computed values of nondimensional secondary variables for SS beam examples.	49
Figure 5.	Nondimensional values of forces and moments by conventional FE method.	49
Figure 6.	SS Beam with Two Symmetric Point Loads and a Central Moment.....	50
Figure 7.	Superposition of two problems – Symmetric and Antisymmetric.....	50
Figure 8.	Cantilever beam with a hinge and two supports.	53
Figure A-1.	Matrix Operations.	62
Figure A-2.	2nd order differential equation.....	63
Figure A-3.	Simply supported beam with 2-elements in half of the beam.....	64

List of Tables

Table 1.	IP Numerical Fluxes*	25
Table 2.	Comparison of DG solution for Various Idealizations ($l = 2h$)	30
Table 3.	Comparison of DG Solution for Various Idealizations ($l = 2h$)	32
Table 4.	IP Numerical Fluxes for Euler-Bernoulli Beam Problems	36
Table 5.	Values of φ_j and $\frac{d\varphi_j}{dx}$	36
Table 6.	Comparison of DG Solution for Cantilever Problem – 2-Element Solution	44
Table 7.	DG solution for a Simply Supported Beam – 2-Element Solution in Half the Beam	47
Table 8.	DG Solution for a Simply Supported Beam – Primary and Secondary Variables	48
Table 9.	DG Solution for Example-3: Simply Supported Beam with Complex Loading ..	52
Table 10.	DG Solution for Example-4: Cantilever Beam with a Hinge and Two Supports Subjected to Uniformly Distributed Load, q_0	58

Nomenclature

DG	Discontinuous Galerkin
DG FEM	Discontinuous Galerkin Finite Element Method
FE	Finite Element
FEM	Finite Element Method
GFE	Galerkin FE
IP	Interior Penalty
LHS	Left Hand Side
PG	Petrov-Galerkin
PG FE	Petrov-Galerkin Finite Element
RHS	Right Hand Side
SS	Simply supported
WR	Weighted Residual

Abstract

The purpose of this report is to present details of the Discontinuous Galerkin (DG) Finite Element Method (DG FEM). First the weighted-residual (WR) form is introduced and then the Galerkin Finite Element (FE) (GFE) and the Petrov-Galerkin FE (PG FE) methods are discussed. The details of the implementation of the DG FEM are presented along with two examples, 2nd order and 4th order differential equations, and the performance of the method is discussed.

Introduction

Over the past 7 decades the FEM has been widely applied to a variety of problems in Structural Mechanics and related fields [1-5]. The quality of the FE mesh dictates the quality of the FE solution. Because of this, the current trend is to make the mesh finer and finer, irrespective of whether such refinements are actually needed. Many software products are available to make the meshing easy, quick, and efficient. In some problems, mesh distortions will occur because of large deformations and the accuracy of the FE solutions deteriorates. In such situations remeshing – deleting and adding elements – is needed.

Methods that do not use elements are becoming popular, such as Element Free Galerkin [6], Meshless Petrov-Galerkin [7-8], Smooth Particle Hydrodynamics method and finite volume methods [9], or a FE method that allows construction of enhanced flexibility afforded by discontinuous elements, the DG [10-16] method. There are many advantages of these DG methods [14]:

- DG methods allow choice of approximating polynomials and hence can have high accuracy
- DG methods are highly parallelizable
- Because they are inherently like the FEM, DG methods are well-suited to handle complex configurations
- DG methods can use adaptive strategies since mesh refinement or making the mesh coarser can be achieved without the attention to continuity across element interfaces.

While DG methods have been used in fluid dynamics and finite volume applications, very little literature exists in solid mechanics. The purpose of this report is to explain the details of the DG method by applying the method to structural mechanics problems governed by second order and fourth order differential equations. The purpose is not to illustrate the advantages cited above but rather explain the details of the method. First the weighted residual method, the Galerkin, and the PG methods are explained. Next, the DG method is explained with reference to second and fourth order differential equations. Then the effectiveness of the DG method is demonstrated by application to several beam problems.

Weighted Residual (WR) Methods

The weighted residual (WR) methods aim to find an approximate solution to the governing differential equation by controlling the errors. As an approximate solution is sought, there is an error left in the differential equation for the assumed set of functions (called trial functions). This error is multiplied by a weighting function, called the test function, and integrated over the domain and subsequently this error is minimized.

Second Order Differential Equation: Consider a second order governing differential equation

$$-\frac{d}{dx}\left(a\frac{du}{dx}\right) + b = f; 0 \leq x \leq l \quad (1)$$

with the boundary conditions at $x = 0$, $u = \alpha$; and at $x = l$, $a\frac{du}{dx} = \beta$. In Eq. (1), a , b , α , and β are constants.

An approximate solution for u is sought by minimizing the error using a weight function w as

$$0 = \int_0^l \left[\frac{d}{dx}\left(a\frac{du}{dx}\right) + b - f \right] \cdot w \cdot dx. \quad (2)$$

In the traditional WR methods, a trial function is chosen for u in the form

$$u = \sum_{i=1}^n \varphi_i(x) u_i \quad (3)$$

where n is the number of n -term approximation for the solution. The functions $\varphi_i(x)$, called the trial functions, need to satisfy all the boundary conditions, both kinematic and natural.

Several choices are available for the weight or test function, w in Eq. (2). In the Galerkin method the w 's are chosen to be the same as the φ 's. That is

$$w_j = \varphi_j(x) \quad (4)$$

In the PG method the test functions come from different sources as

$$w_j = \psi_j(x) \quad (5)$$

where $\psi_j(x)$ are independent functions. The requirements on $\psi_j(x)$ are that they need to be linearly independent.

Equations (3) and (4), when substituted into Eq. (2) will lead to a system of linear algebraic equations

$$[A]\{u\} = \{f\} \quad (6)$$

where

$$\{u\} = \{u_1, u_2, \dots, u_n\}^T \text{ and } \{f\} = \{f_1, f_2, \dots, f_n\}^T \quad (7)$$

$$A_{ij} = \int_0^l \psi_i \cdot \left[\frac{d}{dx} \left(a \frac{d\psi_j}{dx} + b \right) - f \right] \cdot dx, \quad (8)$$

and

$$f_i = \int_0^l \psi_i \cdot f \cdot dx. \quad (9)$$

In the traditional method, outlined above, there are two problems. The function $\varphi_i(x)$ needs to satisfy *all* the boundary conditions of the problem and should be differentiable up to the order of derivatives in Eq. (1). Satisfying these two conditions is not always easy.

Galerkin Method: In the GFE, Eq. (2) is used to develop the element equations. The element matrices are assembled just like the conventional FEM and the boundary conditions are applied. The boundary conditions are applied after the element matrices are assembled. As such, the choice of trial functions, $\varphi_i(x)$, is much simplified – the $\varphi_i(x)$ need to be continuous and differential up to the order required by the governing differential equation.

The GFE method is illustrated with the following example.

Example -1: Consider the differential equation

$$\frac{d^2 u}{dx^2} = 2; \quad 0 \leq x \leq l \quad (11)$$

with the boundary conditions at $x = 0$, $u = 0$ and at $x = l$, $\frac{du}{dx} = 1$.

The WR form for an element e , x_e to x_e+h can be written as

$$\int_{x_e}^{x_e+h} \left(\frac{d^2 u}{dx^2} - 2 \right) \cdot w \cdot dx = 0. \quad (12)$$

If Eq. (12) is formulated as a GFE, then the functional choices for u need to be twice differentiable. Hence the following approximation for u is made in terms of the two nodal values of the element as

$$u = \varphi_1 u_1 + \varphi_2 \left[-\left(\frac{du}{dx} \right) \right]_1 + \varphi_3 u_2 + \varphi_4 \left[\left(\frac{du}{dx} \right) \right]_2. \quad (13)$$

The choices $\varphi_j, j=1,4$ are the Hermitian polynomials like those of the beam functions (see ref. 17, Eq. 4.10) as

$$\begin{aligned}\varphi_1 &= 1 - 3\xi^2 + 2\xi^3 & \varphi_2 &= -h(\xi - 2\xi^2 + \xi^3) \\ \varphi_3 &= 3\xi^2 - 2\xi^3 & \varphi_4 &= -h(-\xi^2 + \xi^3)\end{aligned}\quad (14)$$

where $\xi = (x - x_e)/h$. Note that for an element with 2 nodes, only a linear approximation is possible. However, Eq. (12) requires u to be differentiable twice. For this reason, u and $\frac{du}{dx}$ are chosen at each of the nodes. This gives 4 degrees of freedom and a cubic approximation for u is possible. This leads to the choice of the Hermitian polynomials as shape functions shown in Eq. (14).

Noting that the second derivatives of u are needed in Eq. (12). These are obtained as

$$\frac{d^2\varphi_1}{dx^2} = \frac{1}{h^2}(-6 + 12\xi) \quad \frac{d^2\varphi_2}{dx^2} = \frac{(-h)}{h^2}(6\xi - 4) \quad \frac{d^2\varphi_3}{dx^2} = \frac{1}{h^2}(6 - 12\xi) \quad \frac{d^2\varphi_4}{dx^2} = \frac{(-h)}{h^2}(6\xi - 2) \quad (15)$$

In writing Eq. (15) the following chain rule is used.

$$\frac{d}{dx} = \frac{d}{d\xi} \cdot \frac{d\xi}{dx} = \frac{1}{h} \frac{d}{d\xi} \quad \frac{d^2}{dx^2} = \frac{d}{d\xi} \left(\frac{1}{h} \frac{d}{d\xi} \right) \cdot \frac{d\xi}{dx} = \frac{1}{h^2} \frac{d^2}{d\xi^2} \quad (15a)$$

Substituting Eqs. (13) in Eq. (12) gives

$$\int_0^1 \left[\frac{d^2\varphi_1}{dx^2} \cdot u_1 + \frac{d^2\varphi_2}{dx^2} \cdot \left(-\frac{du}{dx}\right)_1 + \frac{d^2\varphi_3}{dx^2} u_2 + \frac{d^2\varphi_4}{dx^2} \cdot \left(-\frac{du}{dx}\right)_2 \right] \cdot w \cdot h \cdot d\xi - \int_0^1 2w \cdot h \cdot d\xi = 0 \quad (16)$$

Using the Galerkin method, ψ_j are chosen as the trial functions φ , Eq. (16) reduces to

$$\int_0^1 \left[\frac{d^2\varphi_1}{dx^2} \cdot u_1 + \frac{d^2\varphi_2}{dx^2} \cdot \left(-\frac{du}{dx}\right)_1 + \frac{d^2\varphi_3}{dx^2} u_2 + \frac{d^2\varphi_4}{dx^2} \cdot \left(-\frac{du}{dx}\right)_2 \right] \cdot \varphi_j \cdot h \cdot d\xi - \int_0^1 2\varphi_j \cdot h \cdot d\xi = 0 \quad (17)$$

for $j=1,2,3$, and 4.

Eq. (17) leads to the element equations

$$[k]\{u\} = \{f\}$$

where

$$[k] = \begin{bmatrix} -6/(5h) & 11/10 & 6/(5h) & 1/10 \\ 1/10 & (-2h)/15 & -1/10 & h/30 \\ 6/(5h) & -1/10 & -6/(5h) & -11/10 \\ 1/10 & h/30 & -1/10 & -2h/15 \end{bmatrix}$$

$$\{u\} = \{u_1 \quad (-\frac{du}{dx})_1 \quad u_2 \quad (-\frac{du}{dx})_2\}^T, \quad (18)$$

and

$$\{f\} = \{h \quad -h^2/6 \quad h \quad h^2/6\}^T.$$

If a 2-element solution is considered, assembling the matrices for the entire domain $0 \leq x \leq l$ i.e., $0 \leq x \leq 2h$, for a model with two equal size elements of length h , leads to (see Figure 1).

$$[k] = \begin{bmatrix} -6/(5h) & 11/10 & 6/(5h) & 1/10 & 0 & 0 \\ 1/10 & (-2h)/15 & -1/10 & h/30 & 0 & 0 \\ 6/(5h) & -1/10 & -12/(5h) & 0 & 6/(5h) & 1/10 \\ 1/10 & h/30 & 0 & (-4h)/15 & -1/10 & h/30 \\ 0 & 0 & 6/(5h) & -1/10 & -6/(5h) & -11/10 \\ 0 & 0 & 1/10 & h/30 & -1/10 & (-2h)/15 \end{bmatrix}$$

$$\{u\} = \{u_1 \quad (-\frac{du}{dx})_1 \quad u_2 \quad (-\frac{du}{dx})_2 \quad u_3 \quad (-\frac{du}{dx})_3\}^T \quad (19)$$

$$\{f\} = \{h \quad -h^2/6 \quad 2h \quad 0 \quad h \quad h^2/6\}^T$$

The boundary conditions are $u_l=0$ and $(\frac{du}{dx})_3 = 1$. Substituting these into Eq. (19) gives

$$\begin{bmatrix} (-2h)/15 & -1/10 & h/30 & 0 \\ -1/10 & -12/(5h) & 0 & 6/(5h) \\ h/30 & 0 & (-4h)/15 & -1/10 \\ 0 & 6/(5h) & -1/10 & -6/(5h) \end{bmatrix} \begin{bmatrix} (-\frac{du}{dx})_1 \\ u_2 \\ (-\frac{du}{dx})_2 \\ u_3 \end{bmatrix} = \begin{bmatrix} 0 \\ 1/10 \\ h/30 \\ -11/10 \end{bmatrix} + \begin{bmatrix} -h^2/6 \\ 2h \\ 0 \\ h \end{bmatrix}. \quad (20)$$

Solving the system of equations,

$$\begin{bmatrix} (-\frac{du}{dx})_1 \\ u_2 \\ (-\frac{du}{dx})_2 \\ u_3 \end{bmatrix} = \begin{bmatrix} 4h - 1 \\ h - 3h^2 \\ 2h - 1 \\ 2h - 4h^2 \end{bmatrix}. \quad (21)$$

The exact solution of this problem in Eq. (11) is

$$u = x^2 + (1 - 4h)x.$$

The exact solution is reproduced by the 2-element GFE method solution in Eq. (21) at the nodes 1, 2, and 3.

PG Method: As mentioned previously, in the PG method the weight functions come from different spaces i. e. $\psi_j \neq \varphi_j$. Two choices for the ψ_j are considered for the problem in Eq. (11). The first choice of the ψ_j is

$$\psi_j, \text{ for } j=1 \text{ to } 4 \text{ are } 1, \xi, \xi^2, \xi^3 \quad (22)$$

and the second choice is a completely non-intuitive choice of

$$\psi_j, \text{ for } j=1 \text{ to } 4 \text{ are } \xi^5, \xi^4, \xi^3, \xi^2. \quad (23)$$

These weight functions are used in Eq. (16). For the first choice the element matrices are

$$[k] = \begin{bmatrix} 0 & 1 & 0 & -1 \\ 1/h & 0 & -1/h & -1 \\ 1/h & -1/6 & -1/h & -5/6 \\ 9/(10h) & -1/5 & -9/(10h) & -7/10 \end{bmatrix} \quad (24)$$

$$\{f^*\} = \begin{bmatrix} 2h \\ h \\ 2h/3 \\ h/2 \end{bmatrix}. \quad (25)$$

Consider once again a 2-element solution, each with an element length of h . The assembled matrices will be

$$[k] = \begin{bmatrix} 0 & 1 & 0 & -1 & 0 & 0 \\ 1/h & 0 & -1/h & -1 & 0 & 0 \\ 1/h & -1/6 & -1/h & 1/6 & 0 & -1 \\ 9/(10h) & -1/5 & 1/(10h) & -7/10 & -1/h & -1 \\ 0 & 0 & 1/h & -1/6 & -1/h & -5/6 \\ 0 & 0 & 9/(10h) & -1/5 & -9/(10h) & -7/10 \end{bmatrix} \quad (26)$$

and

$$\{f\} = \begin{bmatrix} 2h \\ h \\ 8h/3 \\ 3h/2 \\ 2h/3 \\ h/2 \end{bmatrix} \quad (27)$$

Prescribing the boundary conditions $u_1 = 0$ and $(\frac{du}{dx})_3 = 1$ gives

$$\begin{bmatrix} 0 & -1/h & -1 & 0 \\ -1/6 & -1/h & 1/6 & 0 \\ -1/5 & 1/(10h) & -7/10 & -1/h \\ 0 & 1/h & -1/6 & -1/h \end{bmatrix} \begin{bmatrix} (-\frac{du}{dx})_1 \\ u_2 \\ (-\frac{du}{dx})_2 \\ u_3 \end{bmatrix} = \begin{bmatrix} 0 \\ -1 \\ -1 \\ -5/6 \end{bmatrix} + \begin{bmatrix} h \\ 8h/3 \\ 3h/2 \\ 2h/3 \end{bmatrix} \quad (28)$$

Solving

$$\begin{bmatrix} \left(-\frac{du}{dx}\right)_1 \\ u_2 \\ \left(-\frac{du}{dx}\right)_2 \\ u_3 \end{bmatrix} = \begin{bmatrix} 4h - 1 \\ h - 3h^2 \\ 2h - 1 \\ 2h - 4h^2 \end{bmatrix}. \quad (29)$$

This solution exactly agrees with the solution obtained using the Galerkin method obtained in Eq. (21).

The second choice of $\xi^5, \xi^4, \xi^3, \xi^2$ as the weight functions, leads to the element matrices

$$[k] = \begin{bmatrix} 5/(7h) & -4/21 & -5/(7h) & -11/21 \\ 4/(5h) & -1/5 & -4/(5h) & -3/5 \\ 9/(10h) & -1/5 & -9/(10h) & -7/10 \\ 1/h & -1/6 & -1/h & -5/6 \end{bmatrix} \quad (30)$$

$$\{f\} = \begin{bmatrix} 2h/6 \\ 2h/5 \\ 2h/4 \\ 2h/3 \end{bmatrix}. \quad (31)$$

Assembling the element matrices and applying boundary conditions $u_1 = 0$ and $\left(\frac{du}{dx}\right)_3 = 1$ leads to

$$\begin{bmatrix} -1/5 & -4/(5h) & -3/5 & 0 \\ -1/5 & -13/(70h) & -187/210 & -5/(7h) \\ -1/6 & -1/(5h) & -31/30 & -4/(5h) \\ 0 & 9/(10h) & -1/5 & -9/10 \end{bmatrix} \begin{bmatrix} \left(-\frac{du}{dx}\right)_1 \\ u_2 \\ \left(-\frac{du}{dx}\right)_2 \\ u_3 \end{bmatrix} = \begin{bmatrix} 0 \\ -11/21 \\ -3/5 \\ -7/10 \end{bmatrix} + \begin{bmatrix} 2h/5 \\ 10h/12 \\ 16h/15 \\ h/2 \end{bmatrix}. \quad (32)$$

Solving

$$\begin{bmatrix} \left(-\frac{du}{dx}\right)_1 \\ u_2 \\ \left(-\frac{du}{dx}\right)_2 \\ u_3 \end{bmatrix} = \begin{bmatrix} 4h - 1 \\ h - 3h^2 \\ 2h - 1 \\ 2h - 4h^2 \end{bmatrix}. \quad (33)$$

This solution agrees exactly with the Galerkin and the PG solution obtained with the first choice of weight functions, showing independence of the choice of the weight functions in the PG method.

Weak Form

As mentioned previously, use of Eq. (2) requires the choice of test functions that are differentiable twice. As the order of the governing differential equation increases, it becomes more difficult to select trial functions that are sufficiently differentiable. This can be avoided by reworking the functional in Eq. (2). Eq. (2) can be transformed by integration by parts as

$$\left[\left(a \frac{du}{dx} + b \right) \cdot w \right]_0^l - \int_0^l \left[a \frac{du}{dx} + b - f \right] \cdot \frac{dw}{dx} dx = 0. \quad (34)$$

In Eq. (34) the order of the derivatives of u is lowered to the first order. As such, any trial function φ_i that is chosen needs to be differentiable once. Also note that the weight function only needs to be differentiable once. Since the weight function w is the analyst's choice and there are no requirements except that they are linearly independent, the function w can be chosen to be differentiable as many times as possible. Also note that the natural boundary condition is now a part of the functional. Thus, trial functions φ_i need to satisfy only the essential boundary conditions. However, if a GFE or PG FE is constructed, the essential boundary condition can be handled *after* the global stiffness is assembled.

The example in Eq. (11) and (12) is reworked using the weak form and the element equations for a general e^{th} element are developed. Recall from Eq. 12 that the W-R form for an element e , x_e to x_e+h can be written as

$$\int_{x_e}^{x_e+h} \left(\frac{d^2 u}{dx^2} - 2 \right) \cdot w \cdot dx = 0.$$

Integrating by parts, one obtains

$$\left[\frac{du}{dx} \cdot w \right]_{x_e}^{x_e+h} - \int_{x_e}^{x_e+h} \frac{du}{dx} \cdot \frac{dw}{dx} dx - \int_{x_e}^{x_e+h} 2 \cdot w dx = 0. \quad (35)$$

Clearly, from Eq. (35) the trial functions for u and weight functions w need to be differentiable once. The trial functions for u are chosen as

$$u^{(e)} = \varphi_1 u_1^{(e)} + \varphi_2 u_2^{(e)} \quad (36)$$

where u_1 and u_2 are nodal values of element e . The choices for φ_1 and φ_2 can be conveniently chosen as

$$\varphi_1 = 1 - \xi \text{ and } \varphi_2 = \xi \quad (37)$$

where $\xi = \frac{x-x_g}{h}$. Note that the φ_1 and φ_2 in Eq. (37) are linear functions of ξ .

Galerkin Method: For the Galerkin method, the test functions w are chosen as the trial functions themselves i.e., $w_1 = 1 - \xi$ and $w_2 = \xi$. Substituting the trial and test functions in Eq. (35) gives

$$\frac{1}{h}(-u_1 + u_2) - \left(\frac{du}{dx}\right)_0 - h = 0$$

and (38)

$$\frac{1}{h}(u_1 - u_2) + \left(\frac{du}{dx}\right)_h - h = 0$$

Rewriting Eq. (38) in the matrix form

$$\frac{1}{h} \begin{bmatrix} 1 & 1 \\ 1 & -1 \end{bmatrix} \begin{bmatrix} u_1 \\ u_2 \end{bmatrix} + \begin{bmatrix} (-du/dx)_0 \\ (du/dx)_h \end{bmatrix} = \begin{bmatrix} h \\ h \end{bmatrix}. \quad (39)$$

Eq. (39) represent the element relationship of an e^{th} element of length h .

Now consider a 2-element model of equal elements of length h (see Figure 1).

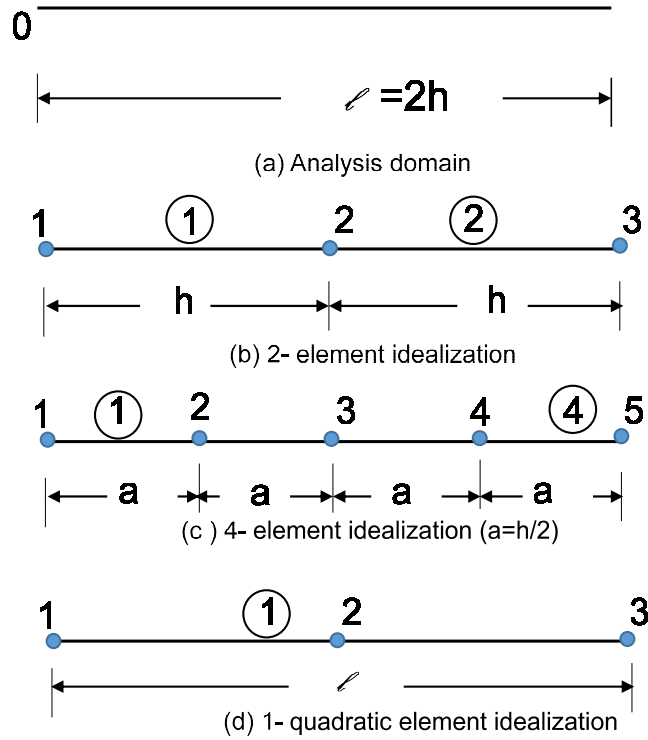


Figure 1. Various idealizations.

Assembling the element matrices gives

$$\frac{1}{h} \begin{bmatrix} -1 & 1 & 0 \\ 1 & -2 & 1 \\ 0 & 1 & -1 \end{bmatrix} \begin{bmatrix} u_1 \\ u_2 \\ u_3 \end{bmatrix} + \begin{bmatrix} (-du/dx)_0 \\ (du/dx)_h - (du/dx)_h \\ (du/dx)_{2h} \end{bmatrix} = \begin{bmatrix} h \\ 2h \\ h \end{bmatrix}. \quad (40)$$

The boundary conditions are $u_1 = 0$ and $(\frac{du}{dx})_{x=l=2h} = 1$. Substituting these boundary conditions in Eq. (40) gives

$$\frac{1}{h} \begin{bmatrix} -2 & 1 \\ 1 & -1 \end{bmatrix} \begin{bmatrix} u_2 \\ u_3 \end{bmatrix} + \begin{bmatrix} 0 \\ 1 \end{bmatrix} = \begin{bmatrix} 2h \\ h \end{bmatrix}. \quad (41)$$

Solving for u_2 and u_3 from Eq. (41),

$$\begin{bmatrix} u_2 \\ u_3 \end{bmatrix} = \begin{bmatrix} h - 3h^2 \\ 2h - 4h^2 \end{bmatrix} \quad (42)$$

Eq. (42) agrees with the exact values given by the Galerkin and PG methods.

A 4-element model with equal size elements of size a is also considered (see Figure 1). The final equations after boundary conditions are

$$\begin{bmatrix} -2 & 1 & 0 & 0 \\ 1 & -2 & 1 & 0 \\ 0 & 1 & -2 & 1 \\ 0 & 0 & 1 & -1 \end{bmatrix} \begin{bmatrix} u_2 \\ u_3 \\ u_4 \\ u_5 \end{bmatrix} = \begin{bmatrix} 2a^2 \\ 2a^2 \\ 2a^2 \\ a^2 - a \end{bmatrix} \quad (43)$$

where $a = h/2$. Solving Eq. (43) gives

$$\begin{bmatrix} u_2 \\ u_3 \\ u_4 \\ u_5 \end{bmatrix} = \begin{bmatrix} h/2 - (7h^2)/4 \\ h - 3h^2 \\ 3h/2 - (15h^2)/4 \\ 2h - 4h^2 \end{bmatrix}. \quad (44)$$

Eq. (44) agrees with the exact values.

PG Method: In the PG method the test functions are different from the trial functions of Eq. (36). Choosing $w_1 = 1$ and $w_2 = \xi$ and substituting trial and test functions in Eq. (35) gives

$$\left(\frac{du}{dx}\right)_h - \left(\frac{du}{dx}\right)_0 - 2h = 0$$

and

$$\frac{1}{h}(u_1 - u_2) + \left(\frac{du}{dx}\right)_h - h = 0. \quad (45)$$

Rewriting Eq. (45) in the matrix form

$$\frac{1}{h} \begin{bmatrix} 0 & 0 \\ 1 & -1 \end{bmatrix} \begin{bmatrix} u_1 \\ u_2 \end{bmatrix} + \begin{bmatrix} (du/dx)_h - (du/dx)_0 \\ (du/dx)_h \end{bmatrix} = \begin{bmatrix} 2h \\ h \end{bmatrix}. \quad (46)$$

Now consider a 2-element model with equal element lengths, h (see Figure 1). Assembling the element matrices gives

$$\frac{1}{h} \begin{bmatrix} 0 & 0 & 0 \\ 1 & -1 & 0 \\ 0 & 1 & -1 \end{bmatrix} \begin{bmatrix} u_1 \\ u_2 \\ u_3 \end{bmatrix} + \begin{bmatrix} (du/dx)_h - (du/dx)_0 \\ (du/dx)_h + (du/dx)_{2h} - (du/dx)_h \\ (du/dx)_{2h} \end{bmatrix} = \begin{bmatrix} 2h \\ h + 2h \\ h \end{bmatrix}. \quad (47)$$

The boundary conditions are $u_1 = 0$ and $(\frac{du}{dx})_{x=l=2h} = 1$. Substituting these boundary conditions in Eq. (47) gives

$$\frac{1}{h} \begin{bmatrix} -1 & 0 \\ 1 & -1 \end{bmatrix} \begin{bmatrix} u_2 \\ u_3 \end{bmatrix} + \begin{bmatrix} 1 \\ 1 \end{bmatrix} = \begin{bmatrix} 3h \\ h \end{bmatrix} \quad (48)$$

Solving for u_2 and u_3 from Eq. (48),

$$\begin{bmatrix} u_2 \\ u_3 \end{bmatrix} = \begin{bmatrix} h - 3h^2 \\ 2h - 4h^2 \end{bmatrix}. \quad (49)$$

These are the same values obtained in Eq. (42) with the Galerkin method.

SIDE BAR-1

Quadratic Element: In this side bar, a quadratic element GFE and PG FE are demonstrated. Consider an element with 3 nodes, two end nodes (1 and 3) and a mid-side node (2) as shown in Figure 1. The field variable u can be approximated by a 2nd degree polynomial. The trial functions for this element are

$$u = \varphi_1 u_1 + \varphi_2 u_2 + \varphi_3 u_3$$

where

$$\varphi_1 = 1 - 3\xi + 2\xi^2; \varphi_2 = 4\xi - 4\xi^2; \varphi_3 = -\xi + 2\xi^2$$

Galerkin method: Because Galerkin method is used, the test functions will be chosen as

$$\psi_1 = 1 - 3\xi + 2\xi^2; \psi_2 = 4\xi - 4\xi^2; \psi_3 = -\xi + 2\xi^2$$

Substituting the φ 's and ψ 's in weak form in Eq. (35) leads to

$$\frac{1}{3l} \begin{bmatrix} 7 & 8 & 1 \\ 8 & -16 & 8 \\ -1 & 8 & -7 \end{bmatrix} \begin{bmatrix} u_1 \\ u_2 \\ u_3 \end{bmatrix} + \begin{bmatrix} -(du/dx)_0 \\ 0 \\ (du/dx)_l \end{bmatrix} = \begin{bmatrix} (2h)/6 \\ (4h)/3 \\ (2h)/6 \end{bmatrix}$$

Substituting the boundary conditions, $u_1 = 0$ and $(du/dx)_l = 1$, leads to

$$\begin{bmatrix} -16 & 8 \\ 8 & -7 \end{bmatrix} \begin{bmatrix} u_2 \\ u_3 \end{bmatrix} = 3l \begin{bmatrix} (4l)/3 \\ (2l)/6 - 1 \end{bmatrix}$$

Solving and recognizing that $l = 2h$ one obtains

$$\begin{bmatrix} u_2 \\ u_3 \end{bmatrix} = \begin{bmatrix} -3h^2 + h \\ -4h^2 + 2h \end{bmatrix}$$

This result is identical to the exact solution.

Petrov-Galerkin method: The test functions for the PGFE are chosen as

$$\psi_1 = 1; \psi_2 = \xi; \psi_3 = \xi^2$$

Substituting the φ 's and ψ 's in weak form in Eq. (35) leads to

$$\frac{1}{l} \begin{bmatrix} 0 & 0 & 0 \\ 1 & 0 & -1 \\ (1/3) & (4/3) & (-5/3) \end{bmatrix} \begin{bmatrix} u_1 \\ u_2 \\ u_3 \end{bmatrix} + \begin{bmatrix} (du/dx)_l - (du/dx)_0 \\ (du/dx)_l \\ (du/dx)_l \end{bmatrix} = \begin{bmatrix} 2l \\ l \\ 2l/3 \end{bmatrix}$$

Substituting the boundary conditions, $u_1 = 0$ and $(du/dx)_l = 1$, leads to

$$\begin{bmatrix} 0 & -1 \\ (4/3) & (-5/3) \end{bmatrix} \begin{bmatrix} u_2 \\ u_3 \end{bmatrix} = \begin{bmatrix} l^2 - l \\ (2l^2)/3 - l \end{bmatrix}$$

Solving and recognizing that $l = 2h$ one obtains

$$\begin{bmatrix} u_2 \\ u_3 \end{bmatrix} = \begin{bmatrix} -3h^2 + h \\ -4h^2 + 2h \end{bmatrix}$$

This result is exactly same as the Galerkin and the exact solutions.

Discontinuous Galerkin Finite Element Method

In the conventional GFE method, continuity of primary variables and reciprocity of tractions across the element interfaces are maintained. In the DG method, as the name implies, the continuity of primary variables across the element boundaries is not explicitly enforced. *As such the number of unknown primary variables is larger compared to the conventional Galerkin method.* In the DG method the governing differential equation is written as two different differential equations of smaller order than the original governing equation. This is very similar to the procedures followed in the mixed methods [2, 9, 17]. Next the weak forms are developed for each of the differential equations. In the weak form, numerical fluxes for the variables in the differential equations are used. Various kinds of numerical fluxes are proposed in the literature and used to connect the variables across the inter-element boundaries [10-16].

Details of the method are illustrated in the section with two problems – a second-order differential equation and a fourth-order differential equation.

Second Order Differential Equation: Consider once again the differential equation

$$\frac{d^2u}{dx^2} = f; \quad 0 \leq x \leq l \quad (50)$$

with the boundary conditions $u_l = 0$ and $\left(\frac{du}{dx}\right) = 1$ at $x = l$.

2-Element Solution: To analyze this problem by the DG method a 2-element idealization is used in the following with equal size elements of length h . The first step in this method is rewrite Eq. (50) as two first order differential equations:

$$\frac{du}{dx} = \tau \quad \text{and} \quad \frac{d\tau}{dx} = f \quad (51)$$

where τ is a new variable. The next step is to develop weak forms for the two equations in Eq. (51). This is accomplished by first writing the WR statements and then by integrating by parts as

$$\int_0^l \left(\frac{du}{dx} - \tau\right) \cdot v \cdot dx = 0$$

and

$$\int_0^l \left(\frac{d\tau}{dx} - f\right) \cdot w \cdot dx = 0 \quad (52)$$

where $v(x)$ and $w(x)$ are the two weight functions.

In the DG method, Eqs. (52) are used to develop matrix equations between the nodal displacements $\{u\}$ and the secondary variables $\{\tau\}$ as

$$[B_1]\{u\} - [W]\{\tau\} = \{0\} \quad (53)$$

and

$$[B_2]\{u\} + [k]\{\tau\} = \{R\}$$

where

$$\{u\} = \left\{ u_1^{(1)} \quad u_2^{(1)} \quad u_1^{(2)} \quad u_2^{(2)} \right\}, \quad (54)$$

$$\text{and } \{\tau\} = \left\{ \tau_1^{(1)} \quad \tau_2^{(1)} \quad \tau_1^{(2)} \quad \tau_2^{(2)} \right\}$$

In the DG method the variables $\{u\}$ and $\{\tau\}$ are listed element by element; i. e. in Eq. (54) the subscript denotes the nodes and the superscript denote the element number. Using the first of Eq. (53), $\{\tau\}$ can be written as

$$\{\tau\} = [\mathbb{M}]^{-1}[B_1]\{u\} \quad (55)$$

and substituting $\{\tau\}$ in the 2nd equation in Eq. (53) gives

$$([B_2] + [k][\mathbb{M}]^{-1}[B_1])\{u\} = \{R\} \quad (56)$$

Eq. (56) is used to solve for the nodal displacements $\{u\}$. The details of the development of the matrices $[B_1]$, $[\mathbb{M}]$, $[B_2]$, $[k]$, and $\{R\}$ are presented below.

Starting from Eq. (52), the weak forms are developed for each element in the domain $0 \leq x \leq l$ by integration by parts. For each element e, $x_e \leq x \leq x_{e+h}$, the weak form is

$$\hat{u} \cdot v \Big|_{x_e}^{x_e+h} - \int_{x_e}^{x_e+h} u \frac{dv}{dx} dx - \int_{x_e}^{x_e+h} \tau \cdot v \cdot dx = 0 \quad (57)$$

$$\hat{t} \cdot w \Big|_{x_e}^{x_e+h} - \int_{x_e}^{x_e+h} \tau \frac{dw}{dx} dx - \int_{x_e}^{x_e+h} f \cdot w \cdot dx = 0 \quad (58)$$

and similar equations for each of the elements in the domain.

In Eqs. (57) and (58), \hat{u} and \hat{t} are called numerical fluxes which are approximations for u and τ at the ends of element e. There are three possibilities, Γ , at the ends of the element: Γ_D , Γ_N , and Γ_h . Here Γ_D is a location where essential boundary condition is prescribed, Γ_N is a location where natural boundary conditions are prescribed, and Γ_h is a location where neither essential nor natural boundary conditions are prescribed, i.e., these are internal points. At these Γ_h locations, the average and jump operators (denoted by $\{u\}$ and $[[u]]$, respectively), are defined in the DG method as

$$\{u\} = \frac{1}{2}(u_{n^-} + u_{n^+}) \text{ and } [[u]] = u_{n^-}(n_1) + u_{n^+}(n_2) \quad (59)$$

and similar definitions for τ . In Eq. (59) u_{h-} and u_{h+} are the left and right side values of u at $x=h$ and n_1 and n_2 are the direction cosines from the left and right sides. Note that $n_1 = 1$ and $n_2 = -1$. The jump operator turns out to be $[[u]] = u_{h-} - u_{h+}$. As mentioned previously, different numerical fluxes have been proposed by various authors [11,12,14]. In this report, interior penalty (IP) numerical fluxes are used and are presented in Table 1 [14].

The next step is to assume trial functions for u and τ and test functions for v and w as

$$u^{(\varepsilon)} = \varphi_1 u_1^{(\varepsilon)} + \varphi_2 u_2^{(\varepsilon)} \text{ and } \tau^{(\varepsilon)} = \varphi_1 \tau_1^{(\varepsilon)} + \varphi_2 \tau_2^{(\varepsilon)} \quad (60)$$

where u_1, u_2 and τ_1, τ_2 are the nodal values of u and τ , respectively, at the two ends of the element, and $u^{(\varepsilon)}$ and $\tau^{(\varepsilon)}$ inside the element are interpolated using the shape functions φ_1 and φ_2 . The shape functions are chosen to be linear as $\varphi_1 = 1 - \xi$ and $\varphi_2 = \xi$.

Also note that the same linear functions φ_1 and φ_2 are used for u and τ in Eq. (60). Since the Galerkin method is used, the test functions φ_1 and φ_2 are the same as the trial functions φ_1 and φ_2 , and the test functions v_2 and w_2 are the same as the trial function φ_2 .

Element-1: Substituting the φ 's in the weak form of Eq. (57) and recognizing that the ends of the element can be written as h and θ , leads to

$$\begin{aligned} (\hat{u} \cdot v_1)_h - (\hat{u} \cdot v_1)_\theta + \frac{1}{2}(u_1^{(1)} + u_2^{(1)}) - \left(\frac{h}{3} \cdot \tau_1^{(1)} + \frac{h}{6} \cdot \tau_2^{(1)}\right) &= 0, \text{ for } j = 1, \\ (\hat{u} \cdot v_2)_h - (\hat{u} \cdot v_2)_\theta - \frac{1}{2}(u_1^{(1)} + u_2^{(1)}) - \left(\frac{h}{6} \cdot \tau_1^{(1)} + \frac{h}{3} \cdot \tau_2^{(1)}\right) &= 0, \text{ for } j = 2, \end{aligned} \quad (61)$$

where $u_1^{(1)}, u_2^{(1)}, \tau_1^{(1)}$, and $\tau_2^{(1)}$ are values of u 's and τ 's, respectively, at the two ends of element 1.

Similarly, Eq. (58) can be written as

$$\begin{aligned} (\hat{t} \cdot w_1)_h - (\hat{t} \cdot w_1)_\theta + \frac{1}{2}(\tau_1^{(1)} + \tau_2^{(1)}) - \frac{fh}{2} &= 0, \text{ for } j = 1 \\ (\hat{t} \cdot w_2)_h - (\hat{t} \cdot w_2)_\theta - \frac{1}{2}(\tau_1^{(1)} + \tau_2^{(1)}) - \frac{fh}{2} &= 0, \text{ for } j = 2. \end{aligned} \quad (62)$$

In Eqs. (61) and (62) there are terms like $(u \cdot v)$ and $(\tau \cdot w)$ at the two ends of the elements. In the DG method, continuity at the inter-element boundaries is NOT explicitly imposed like in the GFE method.

Considering element 1, the values of the test functions v_j can be written as

$$v_1(h) = v_1(\xi = 1) = 0; \quad v_1(0) = v_1(\xi = 0) = 1; \quad v_2(h) = v_2(\xi = 1) = 1;$$

and (63)

$$v_2(0) = v_2(\xi = 0) = 0.$$

Similar values can be written for w_1 and w_2 . With these values, Eqs. (61a) reduce to

$$\begin{aligned} -\hat{u}(0) + \frac{1}{2}(u_1^{(1)} + u_2^{(1)}) - \left(\frac{h}{3}\tau_1^{(1)} + \frac{h}{6}\tau_2^{(1)}\right) &= 0 \\ \hat{u}(h) - \frac{1}{2}(u_1^{(1)} + u_2^{(1)}) - \left(\frac{h}{6}\tau_1^{(1)} + \frac{h}{3}\tau_2^{(1)}\right) &= 0. \end{aligned} \quad (64)$$

Using the IP numerical fluxes in Table 1, $\hat{u}(0)$ is a location of prescribed natural boundary condition, g_D , and $\hat{u}(0) = 0$ as required by the essential boundary condition. That is

$$\hat{u}(h) = \frac{1}{2}(u_{h^-} + u_{h^+}) = \frac{1}{2}(u_2^{(1)} + u_1^{(2)})$$

Substituting these values in Eq. (64) gives

$$\frac{1}{2}(u_1^{(1)} + u_2^{(1)}) - \left(\frac{h}{3}\tau_1^{(1)} + \frac{h}{6}\tau_2^{(1)}\right) = 0 \quad \text{and} \quad -\frac{1}{2}(u_1^{(1)} - u_1^{(2)}) - \left(\frac{h}{6}\tau_1^{(1)} + \frac{h}{3}\tau_2^{(1)}\right) = 0. \quad (65)$$

Substituting the IP numerical fluxes in Eq. (62) leads to

$$-\hat{\tau}(0) + \frac{1}{2}(\tau_1^{(1)} + \tau_2^{(1)}) - \frac{fh}{2} = 0 \quad \hat{\tau}(h) - \frac{1}{2}(\tau_1^{(1)} + \tau_2^{(1)}) - \frac{fh}{2} = 0, \quad (66)$$

where

$$\hat{t}(0) = \tau_1^{(1)} - \frac{\eta}{h_e} u_1^{(1)} \text{ and } \hat{t}(h) = \frac{1}{2} (\tau_2^{(1)} + \tau_1^{(2)}) - \frac{\eta}{h_e} (u_2^{(1)} - u_1^{(2)}). \quad (67)$$

Substituting Eq. (67) in Eq. (66) leads to

$$-\frac{1}{2} (\tau_1^{(1)} - \tau_2^{(1)}) + \frac{\eta}{h_e} u_1^{(1)} - \frac{fh}{2} = 0, \text{ and } -\frac{1}{2} (\tau_1^{(1)} - \tau_1^{(2)}) - \frac{\eta}{h_e} (u_2^{(1)} - u_1^{(2)}) - \frac{fh}{2} = 0. \quad (68)$$

Table 1. IP Numerical Fluxes*

	Γ_h	Γ_D	Γ_N
\hat{u}	$\{u\}$	g_D	u
\hat{t}	$\{\tau\} - \frac{\eta}{h_e} \llbracket u \rrbracket$	$\tau - \frac{\eta}{h_e} (u - g_D)$	g_N

* g_D is the prescribed essential boundary condition, g_N is the prescribed natural boundary condition, and $\frac{\eta}{h_e}$ is the penalty term¹.

Element-2: Following similar procedures as was done for element-1 leads to

$$-\hat{u}(h) + \frac{1}{2} (u_1^{(2)} + u_2^{(2)}) - \left(\frac{h}{2} \tau_1^{(2)} + \frac{h}{6} \tau_2^{(2)} \right) = 0 \quad \hat{u}(2h) - \frac{1}{2} (u_1^{(2)} + u_2^{(2)}) - \left(\frac{h}{6} \tau_1^{(2)} + \frac{h}{3} \tau_2^{(2)} \right) = 0 \quad (69)$$

and

$$-\hat{t}(h) + \frac{1}{2} (\tau_1^{(2)} + \tau_2^{(2)}) - \frac{fh}{2} = 0 \quad \hat{t}(2h) - \frac{1}{2} (\tau_1^{(2)} + \tau_2^{(2)}) - \frac{fh}{2} = 0. \quad (70)$$

¹ The penalty term is used as (η/h_e) in the literature. See references 11,12,14,15, and 16. Hence this definition is retained in this report.

Utilizing the IP numerical fluxes in Table 1 gives

$$\hat{u}(h) = \frac{1}{2}(u_{h^-} + u_{h^+}) = \frac{1}{2}(u_2^{(1)} + u_1^{(2)}) \text{ and } \hat{u}(2h) = u_{2h} = u_2^{(2)},$$

$$\hat{t}(h) = \frac{1}{2}(\tau_1^{(2)} + \tau_2^{(1)}) - \frac{\eta}{h_e}(u_2^{(1)} - u_1^{(2)}),$$

and

$$\hat{t}(2h) = 1,$$

as $x=2h$ is a Γ_N location where $(du/dx)=1$ is prescribed. Substituting these values in Eqs. (69) and (70) gives

$$-\frac{1}{2}(u_2^{(1)} - u_2^{(2)}) - \left(\frac{h}{3}\tau_1^{(2)} + \frac{h}{6}\tau_2^{(2)}\right) = 0 \quad -\frac{1}{2}(u_1^{(2)} - u_2^{(2)}) - \left(\frac{h}{6}\tau_1^{(2)} + \frac{h}{3}\tau_2^{(2)}\right) = 0 \quad (71)$$

and

$$\frac{\eta}{h_e}(u_2^{(1)} - u_1^{(2)}) - \frac{1}{2}(\tau_2^{(1)} - \tau_2^{(2)}) - \frac{fh}{2} = 0, \quad 1 - \frac{1}{2}(\tau_1^{(2)} + \tau_2^{(2)}) - \frac{fh}{2} = 0. \quad (72)$$

Equations (65) and (71) can be written in matrix form as

$$\begin{bmatrix} 1/2 & 1/2 & 0 & 0 \\ -1/2 & 0 & 1/2 & 0 \\ 0 & -1/2 & 0 & 1/2 \\ 0 & 0 & -1/2 & 1/2 \end{bmatrix} \begin{bmatrix} u_1^{(1)} \\ u_2^{(1)} \\ u_1^{(2)} \\ u_2^{(2)} \end{bmatrix} - \begin{bmatrix} h/3 & h/6 & 0 & 0 \\ h/6 & h/3 & 0 & 0 \\ 0 & 0 & h/3 & h/6 \\ 0 & 0 & h/6 & h/3 \end{bmatrix} \begin{bmatrix} \tau_1^{(1)} \\ \tau_2^{(1)} \\ \tau_1^{(2)} \\ \tau_2^{(2)} \end{bmatrix} = \begin{bmatrix} 0 \\ 0 \\ 0 \\ 0 \end{bmatrix}. \quad (73)$$

Similarly, equations (68) and (72) can be written as

$$\frac{\eta}{h_e} \begin{bmatrix} 1 & 0 & 0 & 0 \\ 0 & -1 & 1 & 0 \\ 0 & 1 & -1 & 0 \\ 0 & 0 & 0 & 0 \end{bmatrix} \begin{bmatrix} u_1^{(1)} \\ u_2^{(1)} \\ u_1^{(2)} \\ u_2^{(2)} \end{bmatrix} + \begin{bmatrix} -1/2 & 1/2 & 0 & 0 \\ -1/2 & 0 & 1/2 & 0 \\ 0 & -1/2 & 0 & 1/2 \\ 0 & 0 & -1/2 & -1/2 \end{bmatrix} \begin{bmatrix} \tau_1^{(1)} \\ \tau_2^{(1)} \\ \tau_1^{(2)} \\ \tau_2^{(2)} \end{bmatrix} = \begin{bmatrix} fh/2 \\ fh/2 \\ fh/2 \\ -1 + fh/2 \end{bmatrix}. \quad (74)$$

Equations (73) and (74) can be concisely written as

$$[B_1]\{u\} - [M]\{\tau\} = \{0\}$$

and (75)

$$[B_2]\{u\} + [K]\{\tau\} = \{R\}$$

Note that $[M]$ is a symmetric matrix and has the same form as a ‘mass’ matrix [14]. Also note that this matrix is *always* invertible. Therefore, the $\{\tau\}$ can be eliminated from Eqs. (75) and the final DG final matrix can be written as

$$([B_2] + [K][M]^{-1}[B_1])\{u\} = \{R\} \quad (76)$$

The LHS matrix, in the parenthesis, is in general, not symmetric but is invertible.

The nodal primary variables can be solved using Eq. (76). The current 2-element solution gives

$$\begin{bmatrix} u_1^{(1)} \\ u_2^{(1)} \\ u_1^{(2)} \\ u_2^{(2)} \end{bmatrix} = \begin{bmatrix} 0.0131 \\ -2.0 \\ 1.999 \\ -2.0 \end{bmatrix} \quad (77)$$

for $\eta = 100$. Results for $\eta = 10$ are presented in Table 2 along with the exact values.

4-Element Solution: Consider a 4-element model as shown in Figure 1 with element lengths equal to a , where $a = 2h/4$. With this model the DG method gives the following matrices, similar to Eq. (69) and (70).

$$\begin{bmatrix}
 1/2 & 1/2 & 0 & 0 & 0 & 0 & 0 & 0 \\
 -1/2 & 0 & 1/2 & 0 & 0 & 0 & 0 & 0 \\
 0 & -1/2 & 0 & 1/2 & 0 & 0 & 0 & 0 \\
 0 & 0 & -1/2 & 0 & 1/2 & 0 & 0 & 0 \\
 0 & 0 & 0 & -1/2 & 0 & 1/2 & 0 & 0 \\
 0 & 0 & 0 & 0 & -1/2 & 0 & 1/2 & 0 \\
 0 & 0 & 0 & 0 & 0 & -1/2 & 0 & 1/2 \\
 0 & 0 & 0 & 0 & 0 & 0 & -1/2 & 1/2
 \end{bmatrix}
 \begin{bmatrix}
 u_1^{(1)} \\
 u_2^{(1)} \\
 u_1^{(2)} \\
 u_2^{(2)} \\
 u_1^{(3)} \\
 u_2^{(3)} \\
 u_1^{(4)} \\
 u_2^{(4)}
 \end{bmatrix}
 =$$

(78)

$$\begin{bmatrix}
 a/3 & a/6 & 0 & 0 & 0 & 0 & 0 & 0 \\
 a/6 & a/3 & 0 & 0 & 0 & 0 & 0 & 0 \\
 0 & 0 & a/3 & a/6 & 0 & 0 & 0 & 0 \\
 0 & 0 & a/6 & a/3 & 0 & 0 & 0 & 0 \\
 0 & 0 & 0 & 0 & a/3 & a/6 & 0 & 0 \\
 0 & 0 & 0 & 0 & a/6 & a/3 & 0 & 0 \\
 0 & 0 & 0 & 0 & 0 & 0 & a/3 & a/6 \\
 0 & 0 & 0 & 0 & 0 & 0 & a/6 & a/3
 \end{bmatrix}
 \begin{bmatrix}
 \tau_1^{(1)} \\
 \tau_2^{(1)} \\
 \tau_1^{(2)} \\
 \tau_2^{(2)} \\
 \tau_1^{(3)} \\
 \tau_2^{(3)} \\
 \tau_1^{(4)} \\
 \tau_2^{(4)}
 \end{bmatrix}
 =
 \begin{bmatrix}
 0 \\
 0 \\
 0 \\
 0 \\
 0 \\
 0 \\
 0 \\
 0
 \end{bmatrix}$$

and

$$\frac{\eta}{h_e} \begin{bmatrix} 1 & 0 & 0 & 0 & 0 & 0 & 0 & 0 \\ 0 & -1 & 1 & 0 & 0 & 0 & 0 & 0 \\ 0 & 1 & -1 & 0 & 0 & 0 & 0 & 0 \\ 0 & 0 & 0 & -1 & 1 & 0 & 0 & 0 \\ 0 & 0 & 0 & 1 & -1 & 0 & 0 & 0 \\ 0 & 0 & 0 & 0 & 0 & -1 & 1 & 0 \\ 0 & 0 & 0 & 0 & 0 & 1 & -1 & 0 \\ 0 & 0 & 0 & 0 & 0 & 0 & 0 & 0 \end{bmatrix} \begin{bmatrix} u_1^{(1)} \\ u_2^{(1)} \\ u_1^{(2)} \\ u_2^{(2)} \\ u_1^{(3)} \\ u_2^{(3)} \\ u_1^{(4)} \\ u_2^{(4)} \end{bmatrix} + \begin{bmatrix} -1/2 & 1/2 & 0 & 0 & 0 & 0 & 0 & 0 \\ -1/2 & 0 & 1/2 & 0 & 0 & 0 & 0 & 0 \\ 0 & -1/2 & 0 & -1/2 & 0 & 0 & 0 & 0 \\ 0 & 0 & -1/2 & 0 & 1/2 & 0 & 0 & 0 \\ 0 & 0 & 0 & -1/2 & 0 & 1/2 & 0 & 0 \\ 0 & 0 & 0 & 0 & -1/2 & 0 & 1/2 & 0 \\ 0 & 0 & 0 & 0 & 0 & -1/2 & 0 & 1/2 \\ 0 & 0 & 0 & 0 & 0 & 0 & -1/2 & -1/2 \end{bmatrix} \begin{bmatrix} \tau_1^{(1)} \\ \tau_2^{(1)} \\ \tau_1^{(2)} \\ \tau_2^{(2)} \\ \tau_1^{(3)} \\ \tau_2^{(3)} \\ \tau_1^{(4)} \\ \tau_2^{(4)} \end{bmatrix} = \begin{bmatrix} fa/2 \\ fa/2 \\ fa/2 \\ fa/2 \\ fa/2 \\ fa/2 \\ fa/2 \\ -1 + fa/2 \end{bmatrix} \quad (79)$$

Eliminating $\{\tau\}$ from Eq. (78) and substituting in Eq. (79) as was done for the 2-element solution gives, with $\eta=10$,

$$\begin{bmatrix} u_1^{(1)} \\ u_2^{(1)} \\ u_1^{(2)} \\ u_2^{(2)} \\ u_1^{(3)} \\ u_2^{(3)} \\ u_1^{(4)} \\ u_2^{(4)} \end{bmatrix} = \begin{bmatrix} 0.1063 \\ -1.262 \\ -1.238 \\ -2.001 \\ -1.999 \\ -2.250 \\ -2.250 \\ -2.0 \end{bmatrix}. \quad (80)$$

These values agree well with the exact solution. A solution obtained with $\eta = 100$ is presented in Table 2.

Table 2. Comparison of DG solution for Various Idealizations ($l = 2h$)

Exact Solution is $u = x^2 + (1 - 4h)x$

2-element solution with $h=l$			
x	$\eta = 10$	$\eta = 100$	Exact
0	0.140	0.013	0
h	-2.010, -1.990	-2.000, -1.999	-2.0
$2h$	-2.0	-2.0	-2.0
4-element solution with $h=l$			
0	0.106	0.005	0
$h/2$	-1.262, -1.238	-1.250, -1.250	-1.25
h	-2.001, -1.999	-2.0, -2.0	-2.0
$3h/2$	-2.250, -2.250	-2.250, -2.250	-2.25
$2h$	-2.0	-2.0	-2.0

Example-2: Consider the differential equation

$$\frac{d^2u}{dx^2} = (x + 1) \text{ with } u = 0 \text{ at } x = 0 \text{ and } \frac{du}{dx} = 1 \text{ at } x = l \quad (81)$$

Both 2- and 4- element solutions are attempted. The left-hand side (LHS) of Eq. (79) will remain the same and the right-hand side (RHS) needs to be evaluated with $f = x + 1$. As such, integrals

$$\int_{x_e}^{x_e+h} f \cdot w_1 \, dx \text{ and } \int_{x_e}^{x_e+h} f \cdot w_2 \, dx$$

need to be evaluated. For the 2-element solution the RHS is

$$\begin{bmatrix} \frac{h}{6}(h-3) \\ \frac{h}{6}(h-3) \\ \frac{h}{6}(h-3) \\ -1 + \frac{h}{6}(h-3) \end{bmatrix} \quad (82)$$

and for the 4-element solution the RHS is

$$\begin{bmatrix} \frac{h}{12}\left(3 + \frac{h}{2}\right) \\ \frac{h}{12}\left(3 + \frac{h}{2}\right) \\ \frac{h}{12}\left(3 + \frac{h}{2}\right) \\ \frac{h}{12}\left(3 + \frac{h}{2}\right) \\ \frac{h}{12}\left(3 + \frac{h}{2}\right) \\ \frac{h}{12}\left(3 + \frac{h}{2}\right) \\ \frac{h}{12}\left(3 + \frac{h}{2}\right) \\ \frac{h}{12}\left(3 + \frac{h}{2}\right) \\ -1 + \frac{h}{12}\left(3 + \frac{h}{2}\right) \end{bmatrix} \quad (83)$$

Table 3 presents these solutions along with the exact solution. Excellent agreement is observed between the two sets of solutions.

Table 3. Comparison of DG Solution for Various Idealizations ($l = 2h$)

$$\frac{d^2u}{dx^2} = (x + 1) \text{ with } u = 0 \text{ at } x = 0 \text{ and } \frac{du}{dx} = 1 \text{ at } x = l$$

$$\text{Exact Solution is } u = \frac{x^3}{6} + \frac{x^2}{2} + (1 - 2h - 2h^2)x$$

2-element solution with $h=l$			
x	$\eta = 10$	$\eta = 100$	Exact
0	0.096	0.007	0
h	-2.333, -2.334	-2.333, -2.334	-2.333
$2h$	-2.667	-2.667	-2.667
4-element solution with $h=l$			
0	0.064	0.035	0
$h/2$	-1.360, -1.348	-1.354, -1.354	-1.354
h	-2.332, -2.334	-2.333, -2.334	-2.333
$3h/2$	-2.811, -2.814	-2.812, -2.812	-2.8125
$2h$	-2.667	-2.667	-2.667

Fourth Order Differential Equation: The DG method is now applied to a 4th order differential equation. The governing differential equation for an Euler-Bernoulli beam problem is (see Figure 2)

$$EI \frac{d^4w}{dx^4} = q \quad (84)$$

where w is the deflection $w=w(x)$, $q = q(x)$ is the distributed loading on the beam and EI is the flexural rigidity of the beam. The beam is subjected to essential boundary conditions on w and θ

(slope of the deflection curve) at either end of the beam and natural boundary conditions on the moment M and shear force V . The relationships between w , M , and V are (see Reddy [18] Page 76).

$$\theta = -\frac{dw}{dx}, M = EI \frac{d^2w}{dx^2}, \text{ and } V = EI \frac{d^3w}{dx^3}. \quad (85)$$

Following similar procedure as in the 2nd order equation, Eq. (84) is written as two 2nd order equations as

$$EI \frac{d^2w}{dx^2} = M$$

and (86)

$$\frac{d^2M}{dx^2} = q.$$

The WR form of Eq. (86) is set up using weight functions $\alpha(x)$ and $\beta(x)$ as

$$\int_0^l (EI \frac{d^2w}{dx^2} - M) \cdot \alpha \cdot dx = 0$$

and (87)

$$\int_0^l (\frac{d^2M}{dx^2} - q) \cdot \beta \cdot dx = 0$$

where l is the beam length. For an n -element idealization, the WR statement of Eq. (84) for each element of length h will be

$$\int_{x_e}^{x_e+h} (EI \frac{d^2w}{dx^2} - M) \cdot \alpha \cdot dx = 0$$

and (88)

$$\int_{x_e}^{x_e+h} (\frac{d^2M}{dx^2} - q) \cdot \beta \cdot dx = 0.$$

Equations (88) are integrated by parts twice to transfer the differentiations to the weight functions as

$$EI \frac{dw}{dx} \cdot \alpha|_{x_e}^{x_e+h} - EIw \cdot \frac{d\alpha}{dx}|_{x_e}^{x_e+h} + \int_{x_e}^{x_e+h} EIw \cdot \frac{d^2\alpha}{dx^2} \cdot dx - \int_{x_e}^{x_e+h} M \cdot \alpha \cdot dx = 0 \quad (89)$$

Similarly,

$$\frac{dM}{dx} \cdot \beta|_{x_e}^{x_e+h} - M \cdot \frac{d\beta}{dx}|_{x_e}^{x_e+h} + \int_{x_e}^{x_e+h} M \cdot \frac{d^2\beta}{dx^2} \cdot dx - \int_{x_e}^{x_e+h} q \cdot \beta \cdot dx = 0 \quad (90)$$

Rewriting Eqs., (89) and (90) using numerical fluxes and changing x_e to x_e+h to 0 to h

$$EI \left(\frac{d\hat{w}}{dx} \right) \cdot \alpha|_0^h - EI \hat{w} \cdot \frac{d\alpha}{dx}|_0^h + \int_0^h EI w \cdot \frac{d^2\alpha}{dx^2} \cdot dx - \int_0^h M \cdot \alpha \cdot dx = 0 \quad (91)$$

$$\left(\frac{d\hat{M}}{dx} \right) \cdot \beta|_0^h - \hat{M} \cdot \frac{d\beta}{dx}|_0^h + \int_0^h M \cdot \frac{d^2\beta}{dx^2} \cdot dx - \int_0^h q \cdot \beta \cdot dx = 0. \quad (92)$$

In Eqs. (91) and (92), \hat{w} , $\left(\frac{d\hat{w}}{dx} \right)$, \hat{M} , and $\left(\frac{d\hat{M}}{dx} \right)$ are the numerical fluxes for w , $\left(\frac{dw}{dx} \right)$, M , and $\left(\frac{dM}{dx} \right)$, respectively, at the ends of the e^{th} element. As in the 2nd order equation there are three possibilities for Γ at the two ends of the element e . These are Γ_D , Γ_N , and Γ_h , where Γ_D is the location where essential boundary conditions **w and θ** are prescribed, Γ_N is the location where natural boundary conditions **M and V** are prescribed, and Γ_h is the location where neither boundary condition is prescribed; usually these are interior points in the beam.

As previously mentioned, the IP numerical fluxes are used and are presented in Table 4. The next step is to choose trial and test functions for w and M , and α and β , respectively. As each beam element has two end nodes and w and θ are needed at each end of the element to describe its deformation, a total of 4 degrees of freedom - w_1, θ_1, w_2 and θ_2 , at the two end nodes 1 and 2, respectively, are needed. The trial functions are

$$w = \varphi_1 w_1 + \varphi_2 \theta_1 + \varphi_3 w_2 + \varphi_4 \theta_2 \quad (93)$$

and similar functions for the moment M

$$M = \varphi_1 M_1 + \varphi_2 V_1 + \varphi_3 M_2 + \varphi_4 V_2. \quad (94)$$

The φ_i 's in Eq. (93) and (94) are the well-known Hermitian polynomials shown in Eq. (14). Because a Galerkin method is used, the test functions for α and β will be chosen as φ_j , $j=1,4$. Substituting the trial and test functions in Eq. (87) and (88) leads to

$$\begin{aligned}
& EI \left(\frac{d\hat{w}}{dx} \right)_h \cdot \varphi_j(h) - EI \left(\frac{d\hat{w}}{dx} \right)_0 \cdot \varphi_j(0) - EI(\hat{w})_h \cdot \left[\frac{d\varphi_j}{dx}(h) \right] + EI(\hat{w})_0 \cdot \left[\frac{d\varphi_j}{dx}(0) \right] \\
& + EI \int_0^h (w_1 \varphi_1 + \theta_1 \varphi_2 + w_2 \varphi_3 + \theta_2 \varphi_4) \cdot \frac{d^2 \varphi_j}{dx^2} \cdot dx - \int_0^h (M_1 \varphi_1 + V_1 \varphi_2 + M_2 \varphi_3 + V_2 \varphi_4) \cdot \varphi_j \cdot \\
& dx = 0
\end{aligned} \tag{95}$$

for $j=1,2,3$, and 4, and

$$\begin{aligned}
& \left(\frac{d\tilde{M}}{dx} \right)_h \cdot \varphi_j(h) - \left(\frac{d\tilde{M}}{dx} \right)_0 \cdot \varphi_j(0) - \tilde{M}(h) \cdot \left[\frac{d\varphi_j}{dx}(h) \right] + \tilde{M}(0) \cdot \left[\frac{d\varphi_j}{dx}(0) \right] \\
& + \int_0^h (M_1 \varphi_1 + V_1 \varphi_2 + M_2 \varphi_3 + V_2 \varphi_4) \cdot \frac{d^2 \varphi_j}{dx^2} \cdot dx - \int_0^h q(x) \cdot \varphi_j \cdot dx = 0.
\end{aligned} \tag{96}$$

The derivatives with respect to x are related to derivatives with respect to ξ as

$$\begin{aligned}
& \xi = \frac{(x-x_0)}{h}, \\
& \frac{d}{dx} = \frac{d}{d\xi} \cdot \frac{d\xi}{dx} = \frac{1}{h} \frac{d}{d\xi},
\end{aligned} \tag{97}$$

and

$$\frac{d^2}{dx^2} = \frac{d}{d\xi} \left(\frac{1}{h} \frac{d}{d\xi} \right) = \frac{1}{h^2} \frac{d^2}{d\xi^2}$$

Also note that $dx = h d\xi$. In Eqs. (95) and (96) the values of $\varphi_j(h)$, $\varphi_j(0)$, $\frac{d\varphi_j}{d\xi}(h)$, and $\frac{d\varphi_j}{d\xi}(0)$ are needed. These can be written conveniently, as in Table 5.

Table 4. IP Numerical Fluxes for Euler-Bernoulli Beam Problems

	Γ_h	Γ_D	Γ_N
\widehat{w}	$\{w_h\}$	g_{D_w}	w_h
$\widehat{\theta}$	$\{\theta_h\}$	g_{D_θ}	θ_h
\widehat{M}	$\{M\} - \frac{\eta}{h_e} \llbracket \theta \rrbracket$	$M - \frac{\eta}{h_e} (\theta - g_{D_\theta})$	g_M
$\frac{d\widehat{M}}{dx} = \widehat{V}$	$\left\{ \frac{dM}{dx} \right\} - \frac{\eta}{h_e} \llbracket w \rrbracket$	$V - \frac{\eta}{h_e} (w - g_{D_w})$	g_V

In this Table, g_D is the prescribed essential boundary condition; g_N is the prescribed natural boundary condition; $\frac{\eta}{h_e}$ is the penalty term;

$$\{w_h\} = \frac{1}{2}(w_{h^-} + w_{h^+}); \quad \{\theta_h\} = \frac{1}{2}(\theta_{h^-} + \theta_{h^+});$$

$$\llbracket \theta \rrbracket = \theta_{h^-} n_{h^-} + \theta_{h^+} n_{h^+} = \theta_{h^-} - \theta_{h^+};$$

$$\text{and } \llbracket w \rrbracket = w_{h^-} n_{h^-} + w_{h^+} n_{h^+} = w_{h^-} - w_{h^+}.$$

 Table 5. Values of φ_j and $\frac{d\varphi_j}{dx}$

	φ_j		$\frac{d\varphi_j}{d\xi}$	
	at $h, (\xi = 1)$	at $0, (\xi = 0)$	at $h, (\xi = 1)$	at $0, (\xi = 0)$
Φ_1	0	1	0	0
Φ_2	0	0	0	-h
Φ_3	1	0	0	0
Φ_4	0	0	-h	0

Substituting the trial and test functions into Eq. (95) leads to

$$EI \widehat{w}(h) \frac{1}{h} (-h) = EI \widehat{w}(h) = EI \frac{1}{2} (w_{h^-} + w_{h^+}) = EI \frac{1}{2} (w_2^{(1)} + w_1^{(2)}) \quad (98)$$

$$EI \left(\frac{d\widehat{w}}{dx} \right)_h \cdot \varphi_j(h) - EI \left(\frac{d\widehat{w}}{dx} \right)_0 \cdot \varphi_j(0) - EI \widehat{w}(h) \cdot \frac{1}{h} \cdot \left(\frac{d\varphi_j}{d\xi} \right)_h + EI \widehat{w}(0) \frac{1}{h} \left(\frac{d\varphi_j}{d\xi} \right)_0 + [B_1^{(e)}] \{w^{(e)}\} - [M_1^{(e)}] \{M^{(e)}\} = \{0\} \quad (99)$$

where

$$\{w^{(\varepsilon)}\} = \{w_1 \ \theta_1 \ w_2 \ \theta_2\}^T,$$

$$\{M^{(\varepsilon)}\} = \{M_1 \ V_1 \ M_2 \ V_2\}^T,$$

$$[B_1^{(\varepsilon)}] = EI \begin{bmatrix} -6/(5h) & 1/10 & 6/(5h) & 1/10 \\ 11/10 & -(2h)/15 & -1/10 & h/30 \\ 6/(5h) & -1/10 & -6/(5h) & -1/10 \\ 1/10 & h/30 & -11/10 & -2h/15 \end{bmatrix},$$

and

$$[M_1^{(\varepsilon)}] = \frac{h}{420} \begin{bmatrix} 156 & -22h & 54 & 13h \\ -22h & 4h^2 & -13h & -3h^2 \\ 54 & -13h & 156 & 22h \\ 13h & -3h^2 & 22h & 4h^2 \end{bmatrix}. \quad (100)$$

Substituting the trial and test functions into Eq. (96) leads to

$$\begin{aligned} & \left(\frac{d\hat{M}}{dx}\right)_h \cdot \varphi_j(h) - \left(\frac{d\hat{M}}{dx}\right)_0 \cdot \varphi_j(0) - \hat{M}(h) \cdot \left[\frac{d\varphi_j}{dx}(h)\right] + \hat{M}(0) \cdot \left[\frac{d\varphi_j}{dx}(0)\right] \\ & + [M_2^{(\varepsilon)}]\{M^{(\varepsilon)}\} - \{R^{(\varepsilon)}\} = \mathbf{0} \end{aligned}$$

where

$$[M_2^{(\varepsilon)}] = \begin{bmatrix} -\frac{6}{(5h)} & \frac{1}{10} & \frac{6}{(5h)} & \frac{1}{10} \\ \frac{11}{10} & -\frac{2h}{15} & -\frac{1}{10} & \frac{h}{30} \\ \frac{6}{(5h)} & -\frac{1}{10} & -\frac{6}{(5h)} & -\frac{1}{10} \\ \frac{1}{10} & \frac{h}{30} & -\frac{11}{10} & -\frac{2h}{15} \end{bmatrix},$$

and

$$\{R^{(e)}\} = \begin{bmatrix} h \int_0^h q \varphi_1 \cdot dx \\ h \int_0^h q \varphi_2 \cdot dx \\ h \int_0^h q \varphi_3 \cdot dx \\ h \int_0^h q \varphi_4 \cdot dx \end{bmatrix} \quad (101)$$

As previously mentioned, in the DG FEM, the elements are NOT assembled as in the traditional FEM. Elements are processed individually. The connections between elements are enforced via the four terms involving the numerical fluxes in Eq. (91) and (92) for each value of j . The process is demonstrated in the two examples that are discussed next.

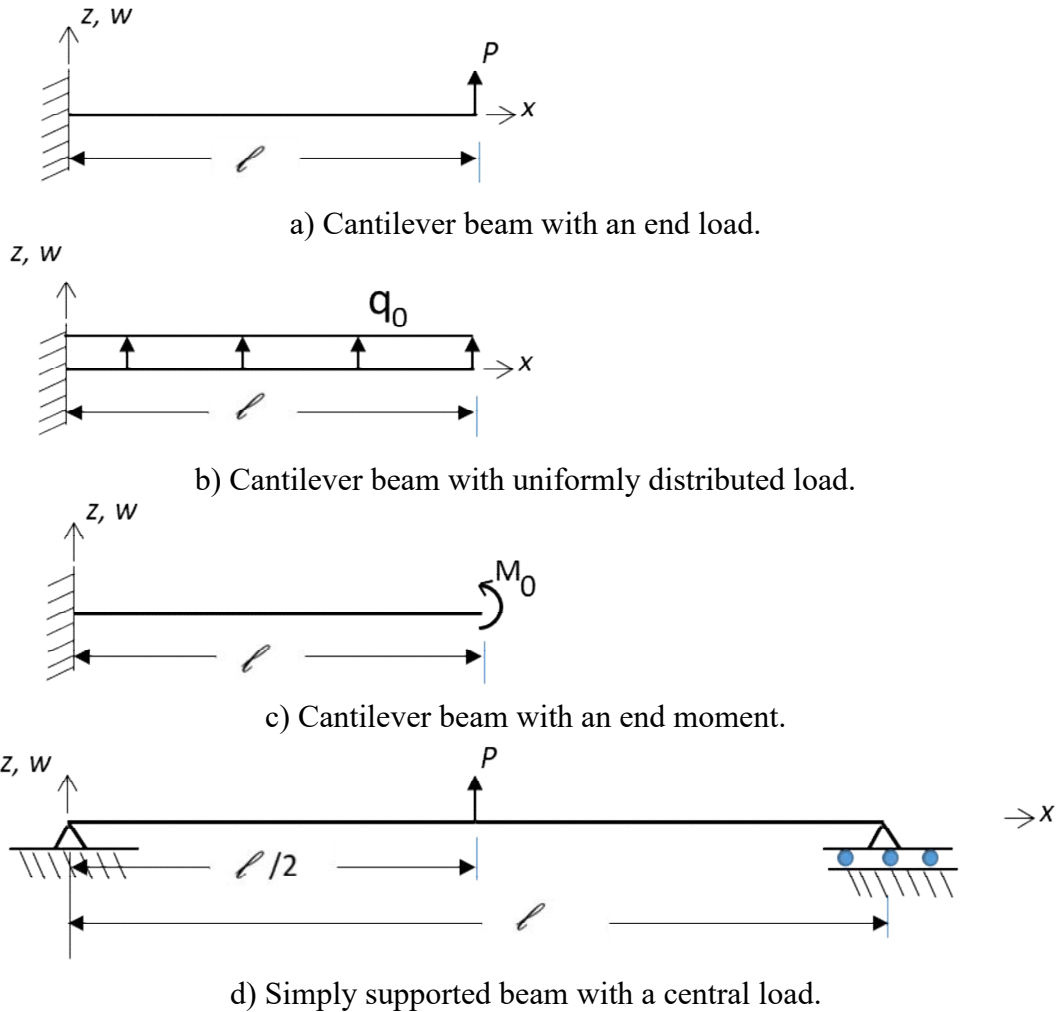


Figure 2. Cantilever and simply supported beam problems studied.

EXAMPLES

Example-1: The first example is a cantilever beam with an end load (see Figure 2(a)). The boundary conditions of the problem are: at $x = 0, w$ and $\frac{dw}{dx} = 0$. At the free end ($x=l$), $V = P$ and $M = 0$. The beam is modeled with 2-elements, each of length h . Equations (99) and (101) need to be applied to each of the elements. Note that all the values in these equations are known except the first 4 terms. These will be evaluated using the numerical fluxes presented in Table 4.

Element-1:

$j=1$: This is a location of $\xi = 0$ and here $\varphi_1 = 1$ (see Table 5). This is a g_D location where $\frac{dw}{dx}$ is prescribed to be zero. Therefore $\frac{d\hat{w}}{dx} = \frac{dw}{dx}(0) = 0$.

$j=2$: This is also a location of $\xi = 0$ and here $\frac{d\varphi_1}{dx} = 1$. This is a g_D location where w is prescribed to be zero. Therefore $\hat{w} = w(0) = 0$.

$j=3$: This is a location of $\xi = 1$ and here $EI \frac{d\hat{w}}{dx}(h)$ needs to be evaluated. From the numerical flux table

$$EI \frac{d\hat{w}}{dx}(h) = -EI \hat{\theta}(h) = -EI \{\theta_h\} = -EI \frac{1}{2} (\theta_{h^-} + \theta_{h^+}) = -EI \frac{1}{2} (\theta_2^{(1)} + \theta_1^{(2)})$$

(In writing the above equation, $\theta = -\frac{dw}{dx}$ is used.)

$j=4$: This is also a location of $\xi = 1$ and here $\frac{d\varphi_4}{d\xi}(h) = 1$.

Therefore

$$EI \hat{w}(h) \frac{1}{h} (-h) = EI \hat{w}(h) = EI \frac{1}{2} (w_{h^-} + w_{h^+}) = EI \frac{1}{2} (w_2^{(1)} + w_1^{(2)})$$

Element-2:

$j=1$: This is a location of $\xi = 0$ and therefore $\varphi_1(0) = 1$.

$$-EI \frac{d\hat{w}}{dx}(0) \cdot 1 = EI \{\hat{\theta}\} = EI \frac{1}{2} (\theta_{h^-} + \theta_{h^-}) = EI \frac{1}{2} (\theta_2^{(1)} + \theta_1^{(2)})$$

$$EI \hat{w}(0) \cdot \frac{1}{h} \cdot (-h) = -EI \hat{w}(0) = -EI \frac{1}{2} (w_{h^-} + w_{h^+}) = -EI \frac{1}{2} (w_2^{(1)} + w_1^{(2)})$$

$j=2$: This is a location of $\xi = 0$ and therefore $\frac{d\varphi_2}{dx}(0) = -h$. Hence

$j=3$: This is a location of $\xi = 1$ and here $\varphi_3(h) = 1$. This is a location of Γ_N , where natural boundary conditions are prescribed. Hence

$$EI \frac{d\hat{w}}{dx}(h) = -EI \hat{\theta}(h) = -EI \theta_h = -EI \theta_2^{(2)}$$

$j=4$: This is a location of $\xi = 1$ and here $\frac{d\varphi_4}{d\xi}(h) = -h$. This gives,

$$EI \hat{w}(h) \cdot \frac{1}{h} \cdot (-h) = EI \hat{w}(h)$$

Because this is a location of Γ_N , $\hat{w}(h) = w(h)$. Thus, this term is $EI w_2^{(2)}$.

Now consider the Eq. (101). Both the elements need to be processed with this equation.

Element-1:

For $j=1$ and 2 , this is a Γ_D location. As such

$$-\frac{d\widehat{M}}{dx}(\mathbf{0}) \cdot \mathbf{1} = -V_1^{(1)} + \frac{\eta}{h_e} (w_1^{(1)} - \mathbf{0})$$

$$\widehat{M}(\mathbf{0}) \cdot \frac{1}{h} \cdot (-h) = -\widehat{M}(\mathbf{0}) = -(M_1^{(1)} - \frac{\eta}{h_e} \cdot \theta_1^{(1)})$$

For $j=3$: $\frac{d\widehat{M}}{dx}(h) \cdot \mathbf{1} = \{V\} - \frac{\eta}{h_e} (w_{h^-} - w_{h^+}) = \frac{1}{2}(V_{h^-} + V_{h^+}) - \frac{\eta}{h_e} (w_{h^-} - w_{h^+})$

$$= \frac{1}{2}(V_2^{(1)} + V_1^{(2)}) - \frac{\eta}{h_e} (w_2^{(1)} - w_1^{(2)})$$

For $j=4$: $-\widehat{M}(h) \cdot \frac{1}{h} \cdot (-h) - \widehat{M}(h) - \{M\} - \frac{\eta}{h_e} [\theta] - \frac{1}{2}(M_2^{(1)} + M_1^{(2)}) - \frac{\eta}{h_e} (\theta_2^{(1)} - \theta_1^{(2)})$

Element-2:

For $j=1$: $-\frac{d\widehat{M}}{dx}(\mathbf{0}) \cdot \mathbf{1} = -\{V\} + \frac{\eta}{h_e} [w] = -\frac{1}{2}(V_2^{(1)} + V_1^{(2)}) + \frac{\eta}{h_e} (w_2^{(1)} - w_1^{(2)})$

For $j=2$: $-\widehat{M}(\mathbf{0}) \cdot \frac{1}{h} \cdot (-h) - \widehat{M}(\mathbf{0}) - \frac{1}{2}\{M\} + \frac{\eta}{h_e} [\theta] - \frac{1}{2}(M_2^{(1)} + M_1^{(2)}) + \frac{\eta}{h_e} (\theta_2^{(1)} - \theta_1^{(2)})$

For $j=3$: $\frac{d\widehat{M}}{dx}(h) \cdot \mathbf{1} = g_V = P$, prescribed load

For $j=4$: $\widehat{M}(h) \cdot \frac{1}{h} \cdot (-h) = \widehat{M}(h) = g_M = \mathbf{0}$, zero moment is prescribed

Using the matrices $[B_1^{(1)}]$, $[\mathfrak{M}_1^{(1)}]$, and $[B_1^{(2)}]$, $[\mathfrak{M}_1^{(2)}]$ and the terms involving numerical fluxes for elements 1 and 2, the global equations can be written as

$$\left(\begin{bmatrix} [B_1^{(1)}] & \mathbf{0} \\ \mathbf{0} & [B_1^{(2)}] \end{bmatrix} + [C_1] \right) \{\delta\} - \begin{bmatrix} [\mathfrak{M}_1^{(1)}] & \mathbf{0} \\ \mathbf{0} & [\mathfrak{M}_1^{(2)}] \end{bmatrix} \{M\} = \{\mathbf{0}\} \quad (102)$$

and

$$\frac{\eta}{h_e} [S] \{\delta\} + \left([C_2] + \begin{bmatrix} [M_2^{(1)}] & 0 \\ 0 & [M_2^{(2)}] \end{bmatrix} \right) \{M\} = \begin{bmatrix} R^{(1)} \\ R^{(2)} \end{bmatrix}, \quad (103)$$

where

$$\{\delta\} = \{w_1^{(1)} \ \theta_1^{(1)} \ w_2^{(1)} \ \theta_2^{(1)} \ w_1^{(2)} \ \theta_1^{(2)} \ w_2^{(2)} \ \theta_2^{(2)}\}^T \quad (104)$$

$$\{M\} = \{M_1^{(1)} \ V_1^{(1)} \ M_2^{(1)} \ V_2^{(1)} \ M_1^{(2)} \ V_1^{(2)} \ M_2^{(2)} \ V_2^{(2)}\}^T,$$

$$[C_1] = EI \begin{bmatrix} 0 & 0 & 0 & 0 & 0 & 0 & 0 & 0 \\ 0 & 0 & 0 & 0 & 0 & 0 & 0 & 0 \\ 0 & 0 & 0 & -\frac{1}{2} & 0 & -\frac{1}{2} & 0 & 0 \\ 0 & 0 & \frac{1}{2} & 0 & \frac{1}{2} & 0 & 0 & 0 \\ 0 & 0 & 0 & \frac{1}{2} & 0 & \frac{1}{2} & 0 & 0 \\ 0 & 0 & -\frac{1}{2} & 0 & -\frac{1}{2} & 0 & 0 & 0 \\ 0 & 0 & 0 & 0 & 0 & 0 & 0 & -1 \\ 0 & 0 & 0 & 0 & 0 & 0 & 1 & 0 \end{bmatrix} \quad (105)$$

$$[C_2] = \begin{bmatrix} 0 & -1 & 0 & 0 & 0 & 0 & 0 & 0 \\ -1 & 0 & 0 & 0 & 0 & 0 & 0 & 0 \\ 0 & 0 & 0 & (1/2) & 0 & (1/2) & 0 & 0 \\ 0 & 0 & (1/2) & 0 & (1/2) & 0 & 0 & 0 \\ 0 & 0 & 0 & -(1/2) & 0 & -(1/2) & 0 & 0 \\ 0 & 0 & -(1/2) & 0 & -(1/2) & 0 & 0 & 0 \\ 0 & 0 & 0 & 0 & 0 & 0 & 0 & 0 \\ 0 & 0 & 0 & 0 & 0 & 0 & 0 & 0 \end{bmatrix} \quad (106)$$

$$[S] = \frac{\eta}{h_e} \begin{bmatrix} 1 & 0 & 0 & 0 & 0 & 0 & 0 & 0 \\ 0 & 1 & 0 & 0 & 0 & 0 & 0 & 0 \\ 0 & 0 & -1 & 0 & 1 & 0 & 0 & 0 \\ 0 & 0 & 0 & -1 & 0 & 1 & 0 & 0 \\ 0 & 0 & 1 & 0 & -1 & 0 & 0 & 0 \\ 0 & 0 & 0 & 1 & 0 & -1 & 0 & 0 \\ 0 & 0 & 0 & 0 & 0 & 0 & 0 & 0 \\ 0 & 0 & 0 & 0 & 0 & 0 & 0 & 0 \end{bmatrix} \quad (107)$$

and

$$\{R\} = \{0 \ 0 \ 0 \ 0 \ 0 \ 0 \ P \ 0\}^T, \quad (108)$$

because $q=0$ and there is a concentrated load at the free end. Equations (102) and (103) can be concisely written as

$$([B_1] + [C_1])\{\delta\} - [\mathbb{W}_1]\{M\} = \{0\}$$

and (109)

$$\frac{\eta}{h_e} [S]\{\delta\} + ([C_2] + [\mathbb{W}_2])\{M\} = \{R\}.$$

Using the first of Eq. (109), $\{M\}$ can be solved as

$$\{M\} = [\mathbb{W}_1]^{-1}([B_1] + [C_1])\{\delta\}. \quad (110)$$

Substituting these values of $\{M\}$ in the second of Eq. (109) gives

$$\left[\frac{\eta}{h_e} [S] + ([C_2] + [\mathbb{W}_2])[\mathbb{W}_1]^{-1}([B_1] + [C_1]) \right] \{\delta\} = \{R\}. \quad (111)$$

Eq. (111) is used to solve for the displacements at all the nodes of the model. The secondary variables $\{M\}$ can be determined from Eq. (110) using the displacements obtained in Eq. (111).

At the element interfaces, the displacements (and moments, M , and shear forces, V) will be discontinuous. In the current model the $w_2^{(1)}$, $w_1^{(2)}$ and $\theta_2^{(1)}$, $\theta_1^{(2)}$ will not be identical. The discrepancy between the values depends on the penalty parameter, $\frac{\eta}{h_e}$, chosen by the user.

The cantilever beam was also analyzed with an end moment and uniformly distributed load. (see Figure 2(b)). The $\{R\}$ vector for an end moment will be

$$\{R\} = \{0 \ 0 \ 0 \ 0 \ 0 \ 0 \ 0 \ M_0\}^T \quad (112)$$

and for uniformly distributed load of intensity q_0 will be

$$\{R\} = \left\{ \frac{q_0 h}{2}, \frac{q_0 h^2}{12}, \frac{q_0 h}{2}, \frac{q_0 h^2}{12}, \frac{q_0 h}{2}, \frac{q_0 h^2}{12}, \frac{q_0 h}{2}, \frac{q_0 h^2}{12} \right\}^T \quad (113)$$

The results for these three loads are presented in Table 6 for three penalty parameters, $\frac{\eta}{h_e} = 10, 100, \text{ and } 1000$. From the results in this table clearly a penalty parameter, $\frac{\eta}{h_e} = 100$ gives accurate results. The current DG 2-element solution agrees extremely well with the exact solution.

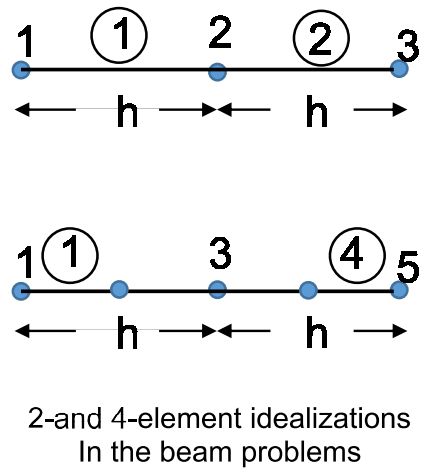


Figure 3. Various idealizations for cantilever and simply supported beam problems.

Table 6. Comparison of DG Solution for Cantilever Problem – 2-Element Solution
(see Figures 2 and 3)

		Concentrated End Load			
x		$\eta = 10$	$\eta = 100$	$\eta = 1000$	Exact
h	$EIw/(Ph^3)$	0.834, 0.832	0.834, 0.832	0.831, 0.835	0.833
h	$EI\theta/(Ph^2)$	-1.495, -1.504	-1.5, -1.5	-1.5, -1.5	-1.5
$2h$	$EIw/(Ph^3)$	2.667	2.667	2.667	2.667

$2h$	$EI\theta/(Ph^2)$	-2.0	-2.0	-2.0	-2.0
Uniformly distributed load q_0					
h	$EIw/(q_0h^4)$	0.709, 0.708	0.709, 0.708	0.703, 0.712	0.708
h	$EI\theta/(q_0h^3)$	-1.162, -1.171	-1.167, -1.167	-1.166, -1.167	-1.167
$2h$	$EIw/(q_0h^4)$	2.0	2.0	2.0	2.0
$2h$	$EI\theta/(q_0h^3)$	-1.333	-1.333	-1.333	-1.333
Concentrated End Moment, M_0					
h	$EIw/(M_0h^2)$	0.5, 0.5	0.5, 0.5	0.5, 0.5	0.5
h	$EI\theta/(M_0h)$	-1.0, -1.0	-1.0, -1.0	-1.0, -1.0	-1.0
$2h$	$EIw/(M_0h^2)$	2.0	2.0	2.0	2.0
$2h$	$EI\theta/(M_0h)$	-2.0	-2.0	-2.0	-2.0

The exact solutions for these problems are:

For concentrated load, P at the free end: $EIw = \frac{P(l-x)^3}{6} - \frac{Pl^2(l-x)}{2} + \frac{Pl^3}{3}$

For a uniformly distributed load q_0 : $EIw = \frac{q_0(l-x)^4}{24} - \frac{q_0l^3(l-x)}{6} + \frac{q_0l^4}{8}$

For concentrated moment, M_0 at the free end: $EIw = \frac{M_0(l-x)^2}{2} - M_0l(l-x) + \frac{M_0l^2}{2} = M_0x^2/2$

Example-2:

The second example considered is a simply supported beam of length l with either a central concentrated load P or a uniformly distributed load q_0 (see Figure 2(d)). Using the symmetries in the problem, only one-half of the beam is modeled using 2 elements, each of length h . The boundary conditions are $w = M = 0$ at $x=0$, and $V = -P/2$ and $\frac{dw}{dx} = 0$ at $x = l/2$. After using numerical fluxes, the matrices $[C_1]$, $[C_2]$, and $[S]$ for this problem are

$$[C_1] = EI \begin{bmatrix} 0 & 1 & 0 & 0 & 0 & 0 & 0 & 0 \\ 0 & 0 & 0 & 0 & 0 & 0 & 0 & 0 \\ 0 & 0 & 0 & -\frac{1}{2} & 0 & -\frac{1}{2} & 0 & 0 \\ 0 & 0 & \frac{1}{2} & 0 & \frac{1}{2} & 0 & 0 & 0 \\ 0 & 0 & 0 & \frac{1}{2} & 0 & \frac{1}{2} & 0 & 0 \\ 0 & 0 & -\frac{1}{2} & 0 & -\frac{1}{2} & 0 & 0 & 0 \\ 0 & 0 & 0 & 0 & 0 & 0 & 0 & 0 \\ 0 & 0 & 0 & 0 & 0 & 0 & 1 & 0 \end{bmatrix} \quad (114)$$

$$[C_2] = \begin{bmatrix} 0 & -1 & 0 & 0 & 0 & 0 & 0 & 0 \\ 0 & 0 & 0 & 0 & 0 & 0 & 0 & 0 \\ 0 & 0 & 0 & (1/2) & 0 & (1/2) & 0 & 0 \\ 0 & 0 & (1/2) & 0 & (1/2) & 0 & 0 & 0 \\ 0 & 0 & 0 & -(1/2) & 0 & -(1/2) & 0 & 0 \\ 0 & 0 & -(1/2) & 0 & -(1/2) & 0 & 0 & 0 \\ 0 & 0 & 0 & 0 & 0 & 0 & 0 & 0 \\ 0 & 0 & 0 & 0 & 0 & 0 & 1 & 0 \end{bmatrix} \quad (115)$$

and

$$[S] = \frac{\eta}{h_e} \begin{bmatrix} 1 & 0 & 0 & 0 & 0 & 0 & 0 & 0 \\ 0 & 0 & 0 & 0 & 0 & 0 & 0 & 0 \\ 0 & 0 & -1 & 0 & 1 & 0 & 0 & 0 \\ 0 & 0 & 0 & -1 & 0 & 1 & 0 & 0 \\ 0 & 0 & 1 & 0 & -1 & 0 & 0 & 0 \\ 0 & 0 & 0 & 1 & 0 & -1 & 0 & 0 \\ 0 & 0 & 0 & 0 & 0 & 0 & 0 & 0 \\ 0 & 0 & 0 & 0 & 0 & 0 & 0 & -1 \end{bmatrix}. \quad (116)$$

The $\{R\}$ vector for the concentrated load will be

$$\{R\} = \{0 \ 0 \ 0 \ 0 \ 0 \ 0 \ \frac{P}{2} \ 0\}^T \quad (117)$$

and for the uniformly distributed load of intensity q_0 will be given by Eq. (113).

The results for displacements for these two loadings are presented in Table 7, again for three penalty parameters, $\frac{\eta}{h_e} = 10, 100, \text{ and } 1000$. Again, clearly $\frac{\eta}{h_e} = 100$ is sufficient to yield accurate results. However, the secondary variables evaluated using Eq. (111) and Eq. (110) are *very inaccurate* for these penalty parameters. Note that the secondary variables are NOT presented in Table 7. (The inaccuracy for the secondary variables is NOT surprising, as the moment and shear force are second and third derivatives of displacements. Displacements need to be very accurate to yield accurate values of moments and shear forces.) With this in mind, the problem is reworked with the penalty parameter set in the range $10^6 \leq \frac{\eta}{h_e} \leq 10^{10}$. The moments and shear forces yielded accurate results, as shown in Table 8 and Figure 4.

Note that the secondary variables can also be computed using the element shape functions ϕ_j of Eq. (14) and Eqs. (85) and (93) as

$$\begin{bmatrix} M_1 \\ V_1 \\ M_2 \\ V_2 \end{bmatrix}^{(e)} = -\frac{EI}{h^3} \begin{bmatrix} -6h & 4h^2 & 6h & 2h^2 \\ 12 & -6h & -12 & -6h \\ 6h & -2h^2 & -6h & 4h^2 \\ 12 & -6h & -12 & -6h \end{bmatrix} \begin{bmatrix} w_1 \\ \theta_1 \\ w_2 \\ \theta_2 \end{bmatrix}^{(e)} \quad (118)$$

These values of the secondary variables are identical to those presented in Table 8.

Table 7. DG solution for a Simply Supported Beam – 2-Element Solution in Half the Beam
(see Figures 2 and 3)

		Concentrated Load, P			
x		$\eta = 10$	$\eta = 100$	$\eta = 1000$	Exact
0	$EI\theta/(Ph^2)$	-1.0	-1.0	-1.0	-1.0
h	$EIw/(Ph^3)$	0.920, 0.913	0.917, 0.916	0.916, 0.918	0.917
h	$EI\theta/(Ph^2)$	-0.745, - 0.754	-0.750, -0.750	-0.750, -0.750	-0.75
$2h$	$EIw/(Ph^3)$	1.333	1.333	1.333	1.333
Exact solution is $EIw = \frac{-Px^3}{12} + \frac{Pl^2x}{16}$					
0	$EI\theta/(q_0h^3)$	-2.667	-2.667	-2.667	-2.667
h	$EIw/(q_0h^4)$	2.373, 2.376	2.376, 2.374	2.371, 2.379	2.375
h	$EI\theta/(q_0h^3)$	-1.830, - 1.828	-1.833, -1.833	-1.833, -1.833	-1.833
$2h$	$EIw/(q_0h^4)$	3.333	3.333	3.333	3.333
Exact solution is $EIw = -\frac{q_0lx^3}{12} + \frac{q_0x^4}{24} + \frac{q_0l^3x}{24}$					

Table 8. DG Solution for a Simply Supported Beam – Primary and Secondary Variables
(2-element solution in half the beam (see Figures 2 and 3))

Element	Primary Variables			Secondary Variables		
	Conc. Load, P*	UDL, q**		Conc. Load, P*	- UDL, q**	
1	\bar{w}_1	1.0E-6	3.5E-6	\bar{M}_1	8.7E-5	-0.0830
	$\bar{\theta}_1$	-1.0	-2.6667	\bar{V}_1	0.5007	1.5033
	\bar{w}_2	0.9167	2.3750	\bar{M}_2	-0.5000	-1.5834
	$\bar{\theta}_2$	-0.75	-1.8333	\bar{V}_2	0.5000	1.5017
2	\bar{w}_1	0.9167	2.3750	\bar{M}_1	-0.5000	-1.5834
	$\bar{\theta}_1$	-0.75	-1.8333	\bar{V}_1	0.5000	0.4988
	\bar{w}_2	1.3333	3.3333	\bar{M}_2	-1.000	-2.0833
	$\bar{\theta}_2$	2.7E-11	-8.3E-8	\bar{V}_2	0.4996	0.4992

*Nondimensional values: $EIw/(Ph^3)$, $EI\theta/(Ph^2)$, and $M/(Ph)$, V/P

**Nondimensional values: $EIw/(qh^4)$, $EI\theta/(qh^3)$, and $M/(qh^2)$, $V/(qh)$

Side Bar-2

In this side bar, forces and moments obtained by the conventional FEM using a 2-node beam element are obtained and compared to the results in Table 8. The beam element stiffness matrix from refs. 2 and 17 (see page 151 Eq. 4.15 of ref. 17) is

$$[K] = \frac{EI}{h^3} \begin{bmatrix} 12 & -6h & -12 & -6h \\ -6h & 4h^2 & 6h & 2h^2 \\ -12 & 6h & 12 & 6h \\ 6h & 2h^2 & 6h & 4h^2 \end{bmatrix} \quad (119)$$

A two-element solution for this stainless steel (SS) beam yields exactly same displacements as shown in Table 8 for both the loading conditions. The nodal forces and moments at the nodes of the two elements can be computed for each element by multiplying the element displacements with the stiffness matrix. The forces and displacements are shown in Figure 5 and they satisfy the reciprocity of tractions at the element interface, $x=h$. The differences between the conventional finite element secondary variables and those of the DG method are due to the conventions of the shear forces and bending moments in the beam theory. The force and moments

shown in Figure 5 satisfy element and global equilibrium conditions.

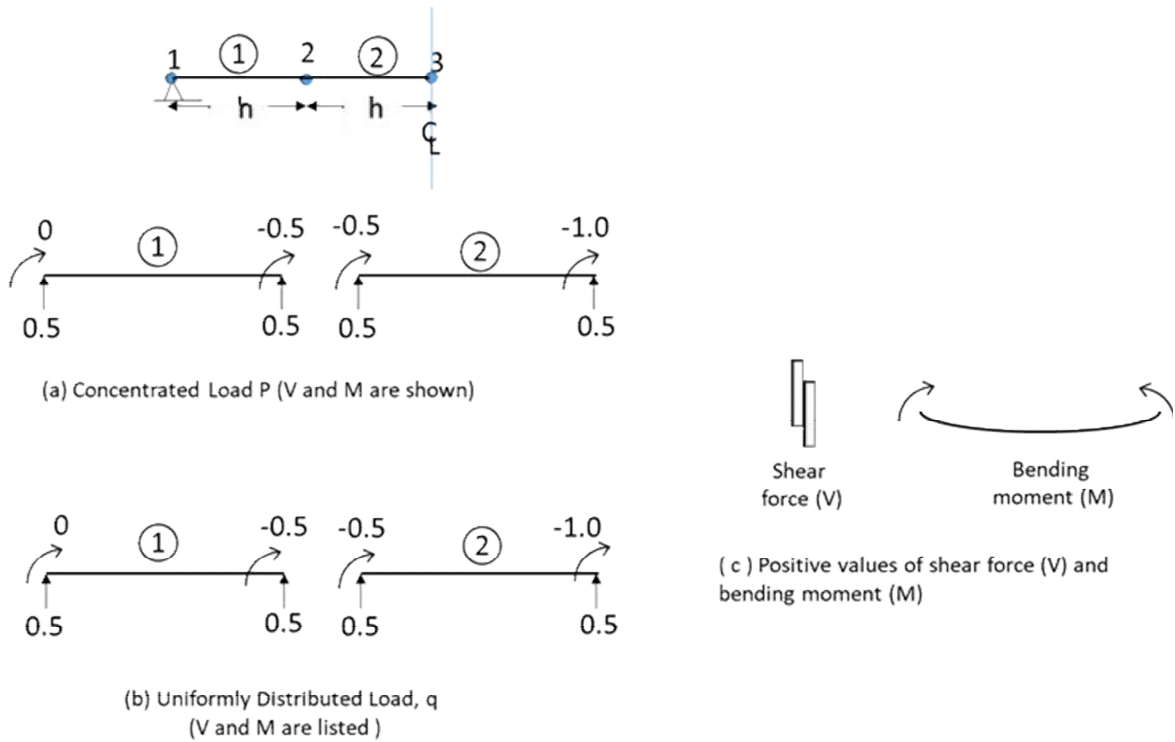


Figure 4. Computed values of nondimensional secondary variables for SS beam examples.

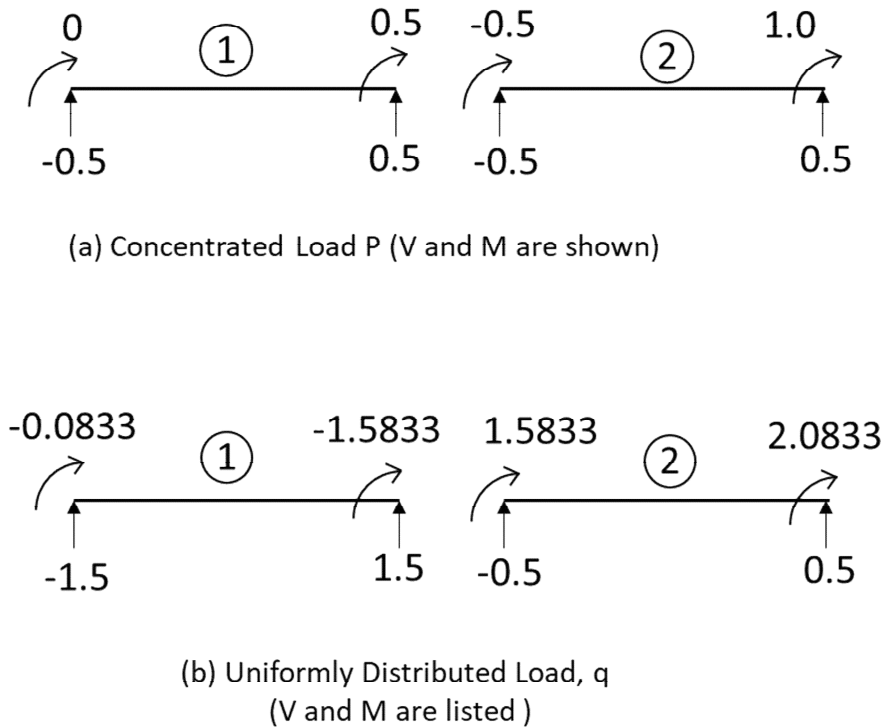


Figure 5. Nondimensional values of forces and moments by conventional FE method.

Example-3:

The third example considered is a SS Beam with two type of loading on the beam as shown in Figure 6. This problem can be easily analyzed by using the principle of superposition. The two loads P are symmetric, but the central moment produces antisymmetric deformations with respect to the center of the beam. As such the beam is analyzed with symmetric loads first and then again with antisymmetric boundary conditions, as shown in Figure 7. The final solution will be obtained by superposition of these two problems.

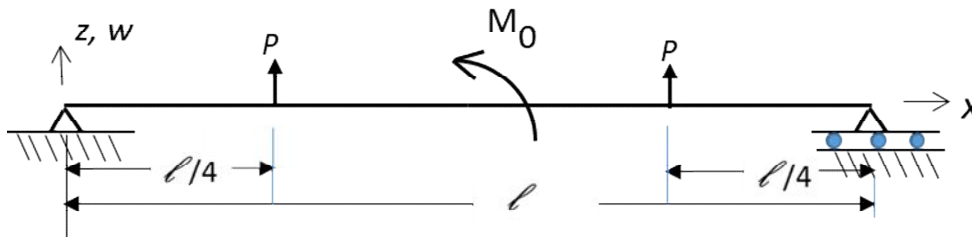


Figure 6. SS Beam with Two Symmetric Point Loads and a Central Moment

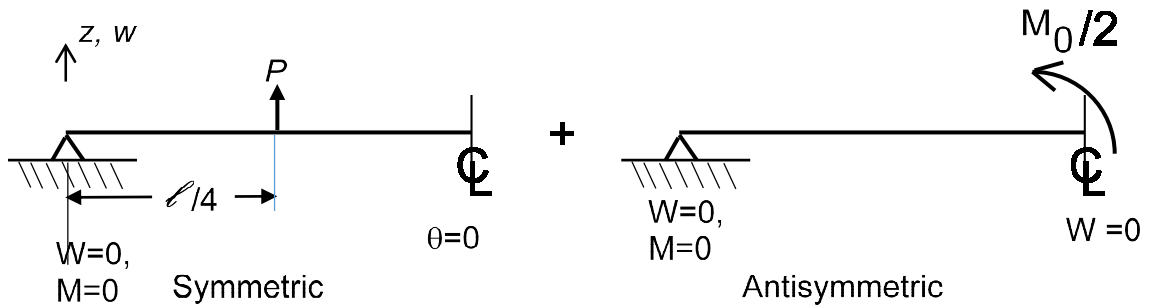


Figure 7. Superposition of two problems – Symmetric and Antisymmetric.

Symmetric problem: This problem is very similar to the problem already worked for the central concentrated load. As such, for a two-element solution, with elements of size h , the matrices $[C_1]$, $[C_2]$, and $[S]$ given in Eqs. (114) and (116) are used. The load vector $\{R\}$ in Eq. (117) needs to be modified. The load is positioned at the boundary of two elements and hence there are three possibilities:

$$\{R\} = \{0 \ 0 \ (P/2) \ 0 \ (P/2) \ 0 \ 0 \ 0\}^T$$

or

$$\{R\} = \{0 \ 0 \ 0 \ 0 \ (P) \ 0 \ 0 \ 0\}^T \tag{120}$$

or

$$\{R\} = \{0 \ 0 \ (P) \ 0 \ 0 \ 0 \ 0 \ 0\}^T$$

The three loadings shown yield identical results for the nodal displacements and are shown in Table 9. Furthermore, any combination of loads that give rise to a total load of P at $x=h$ gives the identical results shown in Table 9.

Antisymmetric problem: This problem is very similar to the symmetric problem but with antisymmetric boundary conditions shown in Figure 7. The matrices $[C_1]$, $[C_2]$, and $[S]$ for this problem are as follows:

$$[C_1] = EI \begin{bmatrix} 0 & 1 & 0 & 0 & 0 & 0 & 0 & 0 \\ 0 & 0 & 0 & 0 & 0 & 0 & 0 & 0 \\ 0 & 0 & 0 & -\frac{1}{2} & 0 & -\frac{1}{2} & 0 & 0 \\ 0 & 0 & \frac{1}{2} & 0 & \frac{1}{2} & 0 & 0 & 0 \\ 0 & 0 & 0 & \frac{1}{2} & 0 & \frac{1}{2} & 0 & 0 \\ 0 & 0 & -\frac{1}{2} & 0 & -\frac{1}{2} & 0 & 0 & 0 \\ 0 & 0 & 0 & 0 & 0 & 0 & 0 & -1 \\ 0 & 0 & 0 & 0 & 0 & 0 & 0 & 0 \end{bmatrix} \quad (121)$$

$$[C_2] = \begin{bmatrix} -1 & 0 & 0 & 0 & 0 & 0 & 0 & 0 \\ 0 & 0 & 0 & 0 & 0 & 0 & 0 & 0 \\ 0 & 0 & (1/2) & 0 & (1/2) & 0 & 0 & 0 \\ 0 & 0 & 0 & (1/2) & 0 & (1/2) & 0 & 0 \\ 0 & 0 & -(1/2) & 0 & -(1/2) & 0 & 0 & 0 \\ 0 & 0 & 0 & -(1/2) & 0 & -(1/2) & 0 & 0 \\ 0 & 0 & 0 & 0 & 0 & 0 & 1 & 0 \\ 0 & 0 & 0 & 0 & 0 & 0 & 0 & 0 \end{bmatrix} \quad (122)$$

and

$$[S] = \frac{\eta}{h_e} \begin{bmatrix} 1 & 0 & 0 & 0 & 0 & 0 & 0 & 0 \\ 0 & 0 & 0 & 0 & 0 & 0 & 0 & 0 \\ 0 & 0 & -1 & 0 & 1 & 0 & 0 & 0 \\ 0 & 0 & 0 & -1 & 0 & 1 & 0 & 0 \\ 0 & 0 & 1 & 0 & -1 & 0 & 0 & 0 \\ 0 & 0 & 0 & 1 & 0 & -1 & 0 & 0 \\ 0 & 0 & 0 & 0 & 0 & 0 & -1 & 0 \\ 0 & 0 & 0 & 0 & 0 & 0 & 0 & 0 \end{bmatrix} \quad (123)$$

The load vector $\{R\}$ is

$$\{R\} = \{0 \ 0 \ 0 \ 0 \ 0 \ 0 \ 0 \ 0 \ M_0/2\}^T \quad (124)$$

The results of the two problems are presented in Table 9 along with the superposed solution.

Table 9. DG Solution for Example-3: Simply Supported Beam with Complex Loading
(2-element solution in half the beam (see Figures 6 and 7))

Element	Symmetric Load, P*	Central Moment M_0^{**}	
1	\bar{w}_1	1.0E-6	2.5E-7
	$\bar{\theta}_1$	-1.5	-0.1667
	\bar{w}_2	1.3333	0.1250
	$\bar{\theta}_2$	-1.0	-0.0417
2	\bar{w}_1	1.3333	0.1250
	$\bar{\theta}_1$	-1.0	-0.0417
	\bar{w}_2	1.8333	2.5E-7
	$\bar{\theta}_2$	1.0E-6	0.3333

*Nondimensional values: $EIw/(Ph^3), EI\theta/(Ph^2)$

**Nondimensional values: $EIw/(M_0h^2), EI\theta/(M_0h)$

Superposed Solution along the length

$$x=0 \quad w = 1.0E - 6 \frac{Ph^3}{EI} + 2.5E - 7 \frac{Mh^2}{EI}$$

$$h \quad w = 1.3333 \frac{Ph^3}{EI} - 0.125 \frac{Mh^2}{EI}$$

$$2h \quad w = 1.8333 \frac{Ph^3}{EI} + 2.5E - 7 \frac{Mh^2}{EI}$$

$$3h \quad w = 1.3333 \frac{Ph^3}{EI} - 0.125 \frac{Mh^2}{EI}$$

$$4h \quad w = 1.0E - 6 \frac{Ph^3}{EI} - 2.5E - 7 \frac{Mh^2}{EI}$$

Example-4:

The fourth example considered is a cantilever beam with two supports and a hinge, as shown in Figure 8. The beam is loaded by a uniformly distributed load, q_0 . The hinge is at $x=h$. The hinge cannot carry moments and hence there is a slope discontinuity at this location, but the deflections are continuous. Two models were developed. The first model had 3 elements while the second model has 5 elements with smaller size elements near the hinge, as shown in Figure 8.

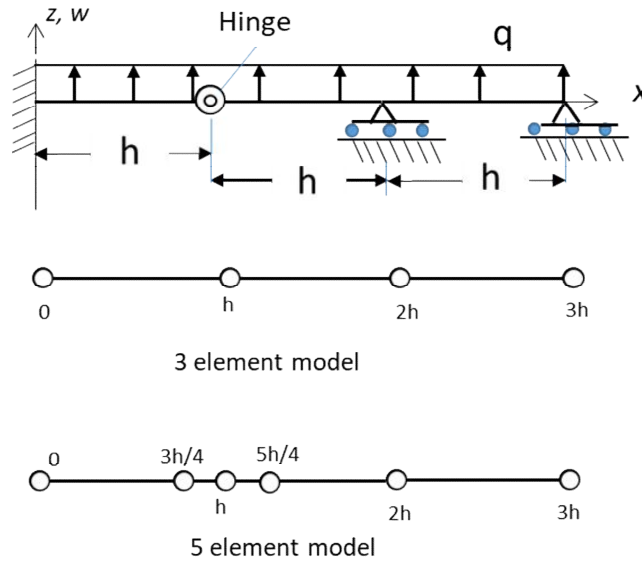


Figure 8. Cantilever beam with a hinge and two supports.

The hinge and the supports at $x=2h$ and $3h$ present new challenges that were not encountered in the earlier examples. As such, details of application of Eqs. (99) and (101) for the 3-element model are presented below.

Element-1:

$j=1$ and 2 : This is a location of $\xi = 0$ and here $\varphi_1 = 1$ and $\frac{d\varphi_1}{dx} = 1$ (see Table 5). This is a \mathcal{G}_D location where $\frac{dw}{dx}$ and w are prescribed to be zero. Therefore $\frac{d\hat{w}}{dx} = \frac{dw}{dx}(0) = 0$ and $\hat{w} = w(0) = 0$. Thus $w_1^{(1)} = \theta_1^{(1)} = 0$

$j=3$: This is a location of $\xi = 1$. This is a hinge location and so at this location the slope is independent. As such $EI \frac{d\hat{w}}{dx}(h) = -\theta_2^{(1)}$.

$j=4$: This is also a location of $\xi = 1$. Here, because of the hinge, w is continuous, i.e., $w_L = w_R$. Thus,

$$EI\hat{w}(h)\frac{1}{h}(-h) = EI\hat{w}(h) = EI\frac{1}{2}(w_{h^-} + w_{h^+}) = EI\frac{1}{2}(w_2^{(1)} + w_1^{(2)})$$

Element-2:

$j=1$: This is a hinge location and so at this location the slope is independent. As such

$$EI\frac{d\hat{w}}{dx}(h) = -\theta_1^{(2)}$$

$j=2$: Here, because of the hinge, w is continuous. Thus

$$w_2^{(1)} = w_1^{(2)}.$$

$j=3$: This is a location of \mathbf{F}_D , the location of the middle support. Hence

$$EI\frac{d\hat{w}}{dx}(2h) = -EI\hat{\theta}(2h) = -EI\theta_{2h} = -EI\theta_2^{(2)}$$

$j=4$: This is a location of \mathbf{F}_D , the location of the middle support. Hence

$$EI\hat{w}(2h) \cdot \frac{1}{h} \cdot (-h) = EI\hat{w}(2h) = EIw_2^{(2)} = 0.$$

Element-3:

$j=1$: This is a location of \mathbf{F}_D , the location of the middle support. Hence

$$EI\frac{d\hat{w}}{dx}(2h) = -\theta_1^{(3)}$$

$j=2$: This is a location of \mathbf{F}_D , the location of the middle support. Hence

$$EI\hat{w}(2h) \cdot \frac{1}{h} \cdot (-h) = EI\hat{w}(2h) = EIw_1^{(3)} = 0$$

$j=3$: This is a location of Γ_D , the location of the middle support. Hence

$$EI \frac{d\hat{w}}{dx}(3h) = -EI\hat{\theta}(3h) = -EI\theta_2^{(3)}$$

$j=4$: This is a location of Γ_D , the location of the middle support. Hence

$$-EI\hat{w}(3h) \cdot \frac{1}{h} \cdot (-h) = EI\hat{w}(3h) = EIw_2^{(3)} = 0$$

Next, the second equation in Eqs. (101) need to be processed for all three elements.

Element-1:

For $j=1$ and 2, this is a Γ_D location. As such,

$$\begin{aligned} -\frac{d\hat{M}}{dx}(0) \cdot 1 &= -V_1^{(1)} + \frac{\eta}{h_e} w_1^{(1)} \\ \hat{M}(0) \cdot \frac{1}{h} \cdot (-h) &= -\hat{M}(0) = -M_1^{(1)} + \frac{\eta}{h_e} \cdot \theta_1^{(1)} \end{aligned}$$

$$\begin{aligned} \text{For } j=3: \frac{d\hat{M}}{dx}(h) \cdot 1 &= \{V\} - \frac{\eta}{h_e} (w_{h^-} - w_{h^+}) = \frac{1}{2}(V_{h^-} + V_{h^+}) - \frac{\eta}{h_e} (w_{h^-} - w_{h^+}) \\ &= \frac{1}{2}(V_2^{(1)} + V_1^{(2)}) - \frac{\eta}{h_e} (w_2^{(1)} - w_1^{(2)}) \end{aligned}$$

$$\text{For } j=4: -\hat{M}(h) \cdot \frac{1}{h} \cdot (-h) = \hat{M}(h) = M_2^{(1)} = 0$$

Element-2:

$$\text{For } j=1: -\frac{d\hat{M}}{dx}(h) \cdot 1 = -\{V\} + \frac{\eta}{h_e} \llbracket w \rrbracket = -\frac{1}{2}(V_2^{(1)} + V_1^{(2)}) + \frac{\eta}{h_e} (w_2^{(1)} - w_1^{(2)})$$

$$\text{For } j=2: -\widehat{M}(3h) \cdot \frac{1}{h} \cdot (-h) = \widehat{M}(3h) = M_2^{(3)} = 0$$

$$\text{For } j=3: \frac{d\widehat{M}}{dx}(2h) \cdot 1 = V_{2h} - \frac{\eta}{h_e} w_{2h} = V_2^{(2)} - \frac{\eta}{h_e} w_2^{(2)}$$

$$\text{For } j=4: -\widehat{M}(2h) \cdot \frac{1}{h} \cdot (-h) = -\widehat{M}(h) = -\frac{1}{2} (M_2^{(2)} + M_1^{(3)}) - \frac{\eta}{h_e} (\theta_2^{(2)} - \theta_1^{(3)})$$

Element-3:

$$\text{For } j=1: \frac{d\widehat{M}}{dx}(3h) \cdot 1 = V(3h) + \frac{\eta}{h_e} w(3h) = V_2^{(3)} - \frac{\eta}{h_e} w_2^{(3)}$$

$$\text{For } j=2: \widehat{M}(2h) \cdot \frac{1}{h} \cdot (-h) = -\widehat{M}(2h) = -\frac{1}{2} (M_2^{(2)} + M_1^{(3)}) + \frac{\eta}{h_e} (\theta_2^{(2)} - \theta_1^{(3)})$$

$$\text{For } j=3: \frac{d\widehat{M}}{dx}(3h) \cdot 1 = V(3h) + \frac{\eta}{h_e} w(3h) = V_2^{(3)} - \frac{\eta}{h_e} w_2^{(3)}$$

$$\text{For } j=4: -\widehat{M}(3h) \cdot \frac{1}{h} \cdot (-h) = \widehat{M}(3h) = M_2^{(3)} = 0$$

The loads $\{R\}$ are

$$\{R\} = \left\{ \frac{q_0 h}{2}, -\frac{q_0 h^2}{12}, \frac{q_0 h}{2}, \frac{q_0 h^2}{12}, \frac{q_0 h}{2}, -\frac{q_0 h^2}{12}, \frac{q_0 h}{2}, \frac{q_0 h^2}{12}, \frac{q_0 h}{2}, -\frac{q_0 h^2}{12}, \frac{q_0 h}{2}, \frac{q_0 h^2}{12} \right\}^T \quad (128)$$

Table 10. DG Solution for Example-4: Cantilever Beam with a Hinge and Two Supports Subjected to Uniformly Distributed Load, q_0

x/h	\bar{w}^*			$\bar{\theta}^*$		
	3-Ele. Model	5-Ele. Model	Exact	3-Ele. Model	5-Ele. Model	Exact
0.75	---	0.1099	0.1099	---	-0.2227	-0.2227
1.0 ⁻	0.1667	0.1667	0.1667	-0.2292	-0.2292	-0.2292
1.0 ⁺	0.1667	0.1667	0.1667	0.1875	0.1875	0.1875
1.25	---	0.1196	0.1198	---	0.1888	0.1888
2.0	0	0	0	0.0833	0.0833	0.0833
3.0	0	0	0	-0.02083	-0.02083	-0.02083

* $\bar{w} = EIw/(q_0 h^4)$ and $\bar{\theta} = EI\theta/(q_0 h^3)$

The exact solution has been obtained and is as follows:

$$\text{For } 0 \leq x \leq h, EIw = -\frac{q_0 h}{16} [31hx^2 - 5x^3] + \frac{q_0(3h-x)^4}{24} + \frac{9}{2}q_0 h^3 x - \frac{27}{8}q_0 h^4$$

$$\text{For } h \leq x \leq 2h, EIw = -\frac{q_0 h}{16} [31hx^2 - 5x^3] + \frac{q_0(3h-x)^4}{24} + \frac{49}{12}q_0 h^3 x - \frac{71}{24}q_0 h^4 \quad (129)$$

$$\text{For } 2h \leq x \leq 3h, EIw = -\frac{q_0 h}{16} [3hx^2 - \frac{x^3}{3}] + \frac{q_0(3h-x)^4}{24} + \frac{7}{24}q_0 h^3 x - \frac{5}{8}q_0 h^4$$

The results in Table 10 show that the both 3- and 5- elements DG solutions reproduced the exact solution accurately.

Concluding Remarks

The details of the Discontinuous Galerkin Finite Element Method (DG FEM) are presented. The weighted-residual form is introduced and the Galerkin FE (GFE) and the Petrov-Galerkin FE (PG FE) methods are discussed. The details of the implementation of the DG FEM are presented along with several examples to demonstrate the performance of the method.

In the DG method, the continuity of the nodal variables across the element interfaces is not explicitly imposed like the GFE or PG FEM; the continuity is imposed through numerical fluxes. In this report the interior penalty (IP) numerical fluxes are used and implemented.

Two simple problems involving second order and fourth differential equations are presented. The GFE, PG FE, and DG FE methods are applied in these problems to demonstrate the differences among the methods. The numerical solutions are compared to the exact solutions to establish the validity of the method. In both problems, a reasonably large penalty parameter is sufficient to yield accurate results.

Next the DG method is demonstrated with reference to a cantilever beam problem with three different loadings, a simply supported beam with three different loadings, and a complex cantilever problem. The DG method is also applied to a continuous beam problem with complex boundary conditions. The results of the DG method are compared to the exact solutions. The DG method yielded accurate results when a large enough penalty parameter was used.

All the computations presented in this report were carried out using Microsoft Excel and the implementation details are presented in the Appendix.

References

1. O. C. Zienkiewicz, and R. L. Taylor, *The Finite Element Method*, Vols. 1 and 2, Fourth Edition, McGraw Hill Publishers, 1989.
2. R. D. Cook, D. S. Malkus, and M. E. Plesha, *Concepts and Applications of Finite Element Analysis*, Third Edition, John Wiley & Sons, 1989.
3. R. H. MacNeal, *Finite Elements: Their Design and Performance*, Marcel Dekker, Inc., 1994.
4. K. L. Bathe, *Finite Element Procedures*, Prentice-Hall, Englewood Cliffs, NJ, 1996.
5. M. A. Crisfield, *Nonlinear Finite Element Analysis of Solids and Structures*, Volume 1, John Wiley & Sons, Chichester, 1991.
6. T. Belytschko, Y. Y. Lu, and L. Gu, Element-free Galerkin Methods, *Int J Numer Methods Eng.* 1994, Vol. 37, pp. 229-256.
7. S. N. Atluri and T. Zhu, A new meshless local Petrov–Galerkin (MLPG) approach. *Comput. Mech.*, 1998, Vol. 23, pp. 117-127.
8. S. N. Atluri, T. L. Zhu, The meshless local Petrov-Galerkin (MLPG) approach for solving problems in elasto-statics, *Comput. Mech.*, 2000, Vol. 25, pp. 169-179
9. S. N. Atluri, *Methods of Computer Modeling in Engineering & the Sciences*, Volume I, Tech Science Press, 2005
10. D. N. Arnold, F. Brezzi, B. Cockburn, and D. Marini, Discontinuous Galerkin methods for elliptic problems, in *Discontinuous Galerkin Methods: Theory, Computation and Applications*, Springer: Berlin, 2000, Vol. 89, pp. 101-129.
11. D. N. Arnold, F. Brezzi, B. Cockburn, and D. Marini, Unified analysis of discontinuous Galerkin methods for elliptic problems, *SIAM Journal on Numerical Analysis*, 2002, Vol. 39, pp.1749–1779.
12. O. C. Zienkiewicz, R. L. Taylor, S. J. Sherwin and J. Peir, On discontinuous Galerkin methods, *Int. J. Numer. Meth. Engng.*, 2003, Vol. 58, pp. 1119–1148
13. P. Castillo, B. Cockburn, I. Perugia, and D. Schotzau, Local discontinuous Galerkin methods for elliptic problems, *Commun. Numer. Meth. Engng.*, 2002, Vol. 18, pp. 69–75
14. P. Castillo, Performance of discontinuous Galerkin methods for elliptic problems, *SIAM Journal on Scientific Computing*, 2002, pp.1-25.

15. L. Dong, T. Yang, K. Wang, and S. N. Atluri, A new Fragile Points method (FPM) in computational mechanics, based on the concepts of point stiffnesses and numerical flux corrections, *Eng. Anal. Bound. Elem.*, 2019, Vol. 107, pp. 124-133.
16. T. Yang, L. Dong, and S. N. Atluri, A simple Galerkin meshless method, the Fragile Points method using point stiffness matrices, for 2D linear elastic problems in complex domains with crack and rupture propagation, *Int. J. Numer. Methods Eng.*, 2020, pp.1–38.
17. J. N. Reddy, *Finite Element Method*, 2nd Edition, McGraw-Hill, Inc.,1993.
18. J. N. Reddy, *Energy and Variational Methods in Applied Mechanics*, John Wiley and Sons, 1984.

Appendix A.

All the matrix operations in this report are performed using Excel spread sheets. This appendix demonstrates how easy it is to perform matrix operations efficiently and accurately using Excel. All the computations involved for the second order differential equation in Eqs. 73-77 are presented. In addition, for a simply supported beam modeled with 2-elements in one half of the beam, the final LHS matrix in Eq. 105 (for a penalty parameter of 100) and its inverse is presented. Next, the two loadings (a central concentrated load and uniformly distributed load) are presented along with the final solution $\{\delta\}$ for these loadings.

Matrix Operations: Figure A-1 demonstrates the matrix operations - matrix inverse, matrix multiplication and addition.

Matrix Inverse: The matrix to be inverted is input in the area occupied by B11 to E14. To capture the inverse the area occupied by G11 to J14 is first highlighted. The next step is to enter the command ‘=MINVERSE(B11:E14)’ and press CTRL and SHIFT together and press ENTER. The inverse will appear in G11 to J14. (On a Mac the command is slightly different - Check the operational manual.)

Note that all the rules of matrix inverses apply to this computation as well. The matrix needs to be square and must have an inverse. If the matrix is singular, errors will appear in the target area.

Matrix multiplication: Two matrices can be multiplied very easily. The matrix in G11 to J14 is multiplied with matrix in B20 to E23. Before this is performed, highlight the area G20 to J23. Then enter the command ‘=MMULT(G11:J14,B20:E23)’ and press CTRL and SHIFT together and press ENTER. The result will appear in G20 to J23.

Note that all the rules of matrix multiplication will apply to this computation as well. The number of columns of the first matrix should be same as the number of rows of the second matrix.

Matrix addition: Two matrices, A and B, need to be added. Here the command is very simple. Matrix A is in the area B27 to E30. The matrix B is the area G27 to J30. To add these matrices together, first highlight the area D34 to G37 and then enter the command ‘=B27:E30+G27:J30’ and press CTRL and SHIFT together and press ENTER. The result will appear in D34 to G37. Note that all the rule of the matrix addition will apply to this computation as well. The two matrices need to be compatible.

2nd Order Differential Equation:

A 2-element solution for the differential equation $\frac{d^2u}{dx^2} = f; 0 \leq x \leq l$ with the boundary conditions $u_l = 0$ and $\left(\frac{du}{dx}\right) = 1$ at $x = l$ is presented in Figure A-2. Equations (73) to (76) with the solution in Eq. (77) are presented in this figure.

Simply-Supported Beam:

A simply supported beam with a 2-element solution in half of the beam is presented in Figure A-3. Only the final matrices are presented, as the model involves 8x8 matrices and they are too large to be presented here.

	A	B	C	D	E	F	G	H	I	J	K		
2													
3													
4													
5													
6		Matrix Operations in EXCEL											
7													
8													
9							Matrix Inverse of Matrix in B11:E14						
10							MINVERSE(B11:E14) and CTRL+SHIFT+ENTER						
11		0.666667	0.333333	0	0		2	-1	0	0			
12		0.333333	0.666667	0	0		-1	2	0	0			
13		0	0	0.666667	0.333333		0	0	2	-1			
14		0	0	0.333333	0.666667		0	0	-1	2			
15													
16													
17													
18							Matrix Multiplication of Two Matrices						
19							MMULT(G11:J14,B20:E23) and CTRL+SHIFT+ENTER						
20		0.5	0.5	0	0		-1.50	-1.00	0.5	0			
21		-0.5	0	0.5	0		1.5	0.5	-1.00	0			
22		0	-0.5	0	0.5		0	1	-0.50	-0.50			
23		0	0	-0.5	0.5		0	-0.50	1	-0.50			
24													
25							Addition of two matrices						
26							Matrix-A			Matrix-B			
27		100	0	0	0		-1.5	-1.00	0.5	0			
28		0	-100	100	0		1.5	0.5	-1.00	0			
29		0	100	100	0		0	1	-0.50	-0.50			
30		0	0	0	0		0	-0.50	1	-0.50			
31													
32													
33							[A]+[B] = (B27:E30+G27:J30) CTRL+SHIFT+ENTER						
34				98.5	-1.00	0.5	0						
35				1.5	-99.50	99	0						
36				0	101	99.5	-0.50						
37				0	-0.50	1	-0.50						
38													
39													
40													

Figure A-1. Matrix Operations.

d²u/dx²=2 with u=0 at x=0 and du/dx=1 at x=l; 2- element idealization								
pen		100		Penalty term (η/h_e); h is length of the element				
h		1						
Matrix \mathcal{M} (see Eq. 73)				Inverse of Matrix \mathcal{M}				
0.333333	0.166667	0.000000	0.000000	4.00	-2.00	0.00	0.00	
0.166667	0.333333	0.000000	0.000000	-2.00	4.00	0.00	0.00	
0.000000	0.000000	0.333333	0.166667	0.00	0.00	4.00	-2.00	
0.000000	0.000000	0.166667	0.333333	0.00	0.00	-2.00	4.00	
Matrix B_1 (Eq. 73)				Inverse of \mathcal{M} times B_1				
0.50	0.50	0.00	0.00	3.00	2.00	-1.00	0.00	
-0.50	0.00	0.50	0.00	-3.00	-1.00	2.00	0.00	
0.00	-0.50	0.00	0.50	0.00	-2.00	1.00	1.00	
0.00	0.00	-0.50	0.50	0.00	1.00	-2.00	1.00	
Matrix K (Eq. 74)				Matrix K times Inverse of \mathcal{M} times B_1				
-0.50	0.50	0.00	0.00	-3.00	-1.50	1.50	0.00	
-0.50	0.00	0.50	0.00	-1.50	-2.00	1.00	0.50	
0.00	-0.50	0.00	0.50	1.50	1.00	-2.00	0.50	
0.00	0.00	-0.50	-0.50	0.00	0.50	0.50	-1.00	
Matrix B-2 (Eq. 74)				LHS of Eq. (76)				
100.0000	0.0000	0.0000	0.0000	97.000000	-1.500000	1.500000	0.000000	
0.0000	-100.0000	100.0000	0.0000	-1.500000	-102.0000	101.000000	0.500000	
0.0000	100.0000	-100.0000	0.0000	1.500000	101.000000	-102.0000	0.500000	
0.0000	0.0000	0.0000	0.0000	0.000000	0.500000	0.500000	-1.000000	
Inverse of LHS of Eq. (76)				Matrix R (RHS of Eq. 74)		Matrix {u} Eq. (77)		
0.010307	-0.000076	0.000076	0.000000	1.000000		0.010307		
-0.000076	-1.002462	-0.997538	-1.000000	1.000000		-2.000076		
0.000076	-0.997538	-1.002462	-1.000000	1.000000		-1.999924		
0.000000	-1.000000	-1.000000	-2.000000	0.000000		-2.000000		

Figure A-2. 2nd order differential equation.

Simply Supported Beam Solutions

LHS of Eq. 105							
-14	-10	18	-3	-36	-5	0	0
-4.3E-14	4	3	1	3	1	0	0
-27	5	-97	9	103	-3	3	-1
414	5	-591	-95	597	105	6	-27
27	1	109	-9	-91	3	-15	1
-414	-3	591	99	-597	-101	5.45E-14	27
0	0	-6	3	-6	3	12	7.11E-15
0	0	-423	31	405	-23	18	-214

Inverse of LHS of Eq. 105							
-0.094475699	-0.08003473	-0.10801	0.006463	-0.09205	0.008283	-0.09175	0.000304
4.62244E-15	2	-1.5	1	-1.5	1	-2	-5E-17
0.001277171	-1.49521175	1.331197	-0.99832	1.334862	-0.99813	1.834877	4.18E-05
-0.19581351	0.810474095	-1.19837	0.999917	-1.18563	1.00737	-1.68391	0.001
-0.001277171	-1.50478825	1.335469	-1.00168	1.331804	-1.00187	1.83179	-4.2E-05
0.19581351	1.189525905	-0.80163	1.000083	-0.81437	0.99263	-1.31609	-0.001
-7.27972E-15	-2	1.833333	-1.5	1.833333	-1.5	2.666667	7.8E-17
-0.054352463	-0.0710237	-0.03712	-0.01119	-0.04809	-0.01007	-0.03836	-0.00458

RHS for Conc. load			RHS for UDL		
0	$w_1^{(1)}$	-0.00459	0.5	$w_1^{(1)}$	-0.18660
0	$\theta_1^{(1)}$	-1	-0.08333	$\theta_1^{(1)}$	-2.66667
0	$w_2^{(1)}$	0.91744	0.5	$w_2^{(1)}$	2.375695
0	$\theta_2^{(1)}$	-0.84195	0.083333	$\theta_2^{(1)}$	-2.199940
0	$w_1^{(2)}$	0.9159	0.5	$w_1^{(2)}$	2.374305
0	$\theta_1^{(2)}$	-0.65805	-0.08333	$\theta_1^{(2)}$	-1.466720
0.5	$w_2^{(2)}$	1.333333	0.5	$w_2^{(2)}$	3.333333
0	$\theta_2^{(2)}$	-0.01918	0.083333	$\theta_2^{(2)}$	-0.083520

Figure A-3. Simply supported beam with 2-elements in half of the beam.